International Journal of Analytical Chemistry

WILEY

RESEARCH ARTICLE OPEN ACCESS

Assessment of Water Quality in El Hamiz Dam Using Pollution Indices and Multivariate Statistics

Amin Chaffai[1] | Hichem Khammar[2] | Nadhir Bouchema[2]

[1]Laboratory of Dynamics and Biodiversity, Faculty of Biological Sciences, University of Science and Technology–Houari Boumediene, Algiers, Algeria | [2]Laboratory of Functional Ecology and Environment, University of Oum El Bouaghi, Oum El Bouaghi, Algeria

Correspondence: Hichem Khammar (hichem.khammar@univ-oeb.dz)

Received: 2 September 2026 | **Revised:** 23 October 2026 | **Accepted:** 3 November 2026

Academic Editor: Arnab Biswas

Keywords: Algeria | eutrophication | freshwater pollution | multivariate analysis | subhumid reservoir | water quality indices

ABSTRACT

This study integrates pollution indices (WPI, NPI, OPI, TLI, TN:TP) with multivariate statistics to assess surface water quality at Algeria's El Hamiz Dam, located in northern Algeria within a subhumid Mediterranean context. Monthly water samples were collected at three sampling stations from January to December 2018 to capture the seasonal dynamics of physicochemical and biological parameters. The indices revealed a clear biphasic seasonal regime. Winter–spring exhibited moderate pollution and hypertrophic status, whereas summer–autumn showed severe deterioration with highly polluted classifications and maximum trophic imbalance (TLI up to 8.76). Spatiotemporal analysis confirmed spatial homogeneity but extreme temporal variability, with spring-to-summer degradation (−190.97%) followed by autumn-to-winter recovery (+64.43%). PCA explained 87% of the total variance, separating organic pollution and trophic gradients from mineralization, and clearly separating winter from summer samples. These patterns suggest that seasonal variability was more pronounced than spatial differences among the monitored stations, highlighting the importance of seasonal monitoring for evaluating reservoir water quality. Such a multi-index approach provides a complementary framework for diagnosing the seasonal dynamics of the subhumid reservoir. The results reveal a chronic hypertrophic condition and seasonal periods of heightened vulnerability, highlighting the critical need for adaptive measures that reduce external nutrient inputs to safeguard this strategic resource in the face of increasing climate and human pressures.

1 | Introduction

Freshwater ecosystems occupy only a small fraction of the Earth's surface but are essential to the support of life and human societies [1]. This over-representation is seen in watercourses such as lakes, rivers, and ponds, which cover only 1% of the planet's surface, yet deliver a multitude of essential ecosystem services. Such services include the provision of drinking water, support for agriculture and fisheries, opportunities for recreation, and maintenance of biodiversity, all of which support human well-being and ecological balance [2]. Anthropogenic pressures on freshwater resources, however, are considerable and have a general impact on both surface water and groundwater, causing a sharp reduction in the quantity and quality of these essential natural resources. Freshwater ecosystems are vanishing at an alarming rate across all continents and major river basins, and they are degrading faster than terrestrial ecosystems [3].

In Algeria, the water crisis is expected to continue to be a major concern during this century, particularly with the increasing scarcity and difficulty in accessing water resources, and the risk of pollution is increasing in many parts of the country [4]. This upcoming crisis is aggravated by the ongoing demographic pressures. A slow increase in fertility rates over the last 2 decades and declining mortality rates for all age groups have contributed

This is an open access article under the terms of the Creative Commons Attribution License, which permits use, distribution and reproduction in any medium, provided the original work is properly cited.

Copyright © 2026 Amin Chaffai et al. *International Journal of Analytical Chemistry* published by John Wiley & Sons Ltd.

to the rapid population growth [5]. Increased demand for water only adds to the stress on already overstressed water resources. There is a tenuous balance between human needs and ecological limits.

The increasing imbalance poses a direct threat to the country's socioeconomic development, which still heavily depends on limited freshwater supplies. However, these critical aquifers, which are the bedrock of agricultural, industrial, and domestic stability, are now under compounding stresses of environmental degradation, unsustainable exploitation, anthropogenic activities, and the impacts of climate change, which suggest a projected decline in the precipitation regimes of these subhumid regions, further aggravating water scarcity [6]. These together threaten the future of current and future generations and threaten long-term water security and economic stability [7, 8]. Dams are therefore very important for the conservation of water as they collect rain and surface flow to ensure a constant supply of water even during dry periods. These infrastructures are of particular importance in semiarid and arid regions for water resource management, as they provide essential storage and regulation mechanisms to alleviate water scarcity [9]. Dams also improve groundwater recharge by allowing water to flow into aquifers. Several studies have demonstrated that the construction of dams results in increasing borehole water levels, therefore proving the efficiency of dams in maintaining underground water resources [9]. Given the complexity of the problems facing freshwater ecosystems, scientific progress on pollution indicators is essential to efficiently monitor, manage, and protect these vital resources for future generations. Such tools include the water pollution index (WPI), Nemerow pollution index (NPI), trophic level index (TLI), and organic pollution index (OPI) [10, 11], which are important in the determination of pollution levels and trophic status over the course of the study period and for the support of sustainable management strategies, especially in water-scarce areas. Global studies emphasize the significance of these indices: They reduce complex water quality data into readily understandable metrics, allowing stakeholders to track trends, communicate risks, and prioritize interventions [10, 12–16].

This study is the first to comprehensively evaluate the pollution status and trophic state of the El Hamiz Dam using a suite of multiple WPIs. The use of a combination of complementary indicators allows an integrated appraisal of water quality in this study, which allows the identification of spatial and temporal patterns of pollution and the classification of the trophic conditions of the dam.

2 | Materials and Methods

2.1 | Study Area

The present study was conducted in the El Hamiz Dam in the Boumerdès Province, approximately 35 km southeast of Algiers, Algeria. The dam is located in the Mitidja Plain and is geographically located at 36°35′59″N latitude and 3°20′50″E longitude (Figure 1). It is located on the Wadi Arbatache in the Lower Kabylia of the Djurdjura mountain range [4]. The El Hamiz Dam was built to meet the water supply needs of a subhumid environment. The dam is essential for the supply of water for domestic consumption and irrigation to the surrounding area. The reservoir was first appraised in 1935 with a total storage capacity of approximately 22 million m^3 and a surface area of 128 ha. The dam structure itself is 45 m high and 222 m long [17]. From a climatic point of view, the region is located in a subhumid bioclimatic stage with a well-defined dry and hot season that lasts approximately 6 months, from May to October. The rest of the year is wet, with an annual average rainfall of 851.9 mm [4]. This seasonal variability is an important driver of hydrological inputs to the reservoir and contributes to its ecological and physicochemical dynamics.

2.2 | Sampling and Analysis Methods

Water samples were collected monthly from 3 sampling stations (HMZ1, HMZ2, and HMZ3) throughout the 12-month monitoring period from January to December 2018, resulting in 12 sampling campaigns. The three stations were selected to represent the main longitudinal sectors of the El Hamiz Reservoir. HMZ1 was located as close as practicable to the main Oued feeding the reservoir, with the aim of capturing the influence of upstream inflow and watershed-derived inputs (e.g., chemical contaminants, geological materials, and nutrients). HMZ2 was located in the central pelagic sector, whereas HMZ3 represented the sector near the dam. This spatial arrangement was designed to provide a consistent comparison between the upstream, central, and near-dam sectors of the reservoir. At each campaign, surface water samples were collected at the 3 stations at a depth of 30 cm. This sampling depth was used to characterize surface water quality. No depth-resolved sampling was conducted in the present study; the collected water were immediately placed in an insulated cooler maintained at 4°C and transferred to the laboratory for analysis within 24 h of collection to ensure the accuracy and reliability of the measured physicochemical parameters. The monthly observations constituted the primary dataset used to characterize the temporal variability of water quality. For seasonal assessment, the monthly observations were grouped into winter, spring, summer, and autumn, and mean values were calculated for each season at each sampling station. This seasonal aggregation was performed to facilitate the comparison of water quality conditions among the four seasons. In situ measurements consisted of temperature (°C), pH, electrical conductivity (EC, µS/cm), DO (mg/L), salinity (‰), and total dissolved solids (TDSs, mg/L), recorded using a portable multiparameter Hanna HI 9829. A Secchi disc was used to measure transparency. The collected water samples were analyzed in the laboratory for major ions and nutrient concentrations (SO_4^{2-}, Cl^-, TH, NO_2^-, NO_3^-, NH_4^+, and PO_4^{3-}) and organic parameters (total suspended solid [TSS], DCO, and biochemical oxygen demand over five days [BOD_5]) according to the standardized analytical methods described by Rodier et al.[18]. Turbidity was determined using a calibrated turbidity meter. Chlorophyll a (Chl a) concentrations were calculated according to the French AFNOR T90-114 standard, which describes the official procedure for the determination of chlorophyll a in water samples.

2.3 | Pollution Assessment Indices

2.3.1 | WPI

The WPI is a composite indicator that integrates multiple physicochemical parameters into a single value to evaluate overall water quality and detect even slight variations in individual measurements. In this study, eleven parameters (pH, NH_4^+, NO_2^-, NO_3^-, PO_4^{3-}, SO_4^{2-}, Cl^-, TH, EC, TDS, and turbidity) were employed for WPI computation. Following the

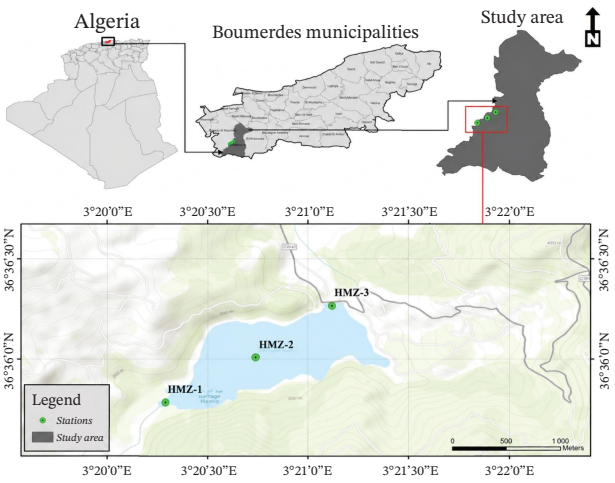

FIGURE 1 | Spatial distribution of sampling stations across the El Hamiz Reservoir, Algeria, HMZ: Hamiz.

approach described by Hossain and Patra [13], the pollution load (PLi) for each parameter was determined as the ratio between the measured concentration (Ci) and the corresponding permissible standard (Si). The WPI value was calculated as the arithmetic mean (1) and (2) of all (PL*i*) values:

$$\mathrm{PL}i = \frac{\mathrm{ci}}{\mathrm{si}}, \tag{1}$$

$$\mathrm{WPI} = \sum \frac{\mathrm{PLi}}{n}, \tag{2}$$

where n represents the total number of parameters. Higher WPI values indicate greater deviations from standard limits and, therefore, higher levels of pollution. The WPI was interpreted according to the classification proposed by Hossain and Patra [13]: $\mathrm{WPI} < 0.50$ indicates excellent water quality; $0.50 \leq \mathrm{WPI} < 0.75$ indicates good water quality; $0.75 \leq \mathrm{WPI} \leq 1.00$ indicates moderately polluted water; and $\mathrm{WPI} > 1.00$ indicates highly polluted water. (Table 1)

2.3.2 | NPI

The NPI was used to assess the overall water quality status of the El Hamiz Dam. This index was first developed by Nemerow [19] as a comprehensive method to assess stream pollution by integrating multiple water quality parameters into a single composite value. Each parameter was first normalized to the corresponding water quality standard to give a single pollution index value (*Pi*):

$$Pi = \frac{Ci}{Si}, \tag{3}$$

where *Ci* is the measured concentration of the parameter and *Si* is the corresponding standard or guideline value.

The average pollution index (P_{avg}) and the maximum pollution index (P_{max}) among all parameters were calculated. The final NPI value was derived as follows:

$$\mathrm{NPI} = \sqrt{\frac{P_{\mathrm{avg}}^2 + P_{\mathrm{max}}^2}{2}}. \tag{4}$$

According to Nemerow [19], the classification of water quality based on the NPI is shown in Table 2.

2.3.3 | Water Quality Variability Across Space and Time in Hamiz Reservoir

To evaluate the intensity of temporal and spatial variability of water quality in the Hamiz reservoir, two complementary indicators were used: temporal change rate (T) and spatial change rate (S). The first one measures the relative change of the NPI over successive time intervals and the second one over different monitoring stations.

The temporal change rate (T) was used to evaluate seasonal dynamics and is defined as follows:

$$T = \frac{Gt_1 - Gt_2}{Gt_1} * 100, \tag{5}$$

where Gt_1 is the NPI at the beginning of a given period and Gt_2 is the corresponding NPI at the end of that period. A positive value of T denotes an improvement in water quality, whereas a negative value reflects deterioration.

Similarly, the spatial change rate (S) characterizes differences in water quality between stations and is expressed as

$$S = \frac{Gs_1 - Gs_2}{Gs_1} * 100, \tag{6}$$

where Gs_1 and Gs_2 correspond to the NPI values at the start and end points of the spatial comparison, respectively. As with the temporal metric, positive values of S indicate better conditions relative to the reference station, while negative values highlight deterioration.

Thresholds were used to simplify interpretation, in agreement with previous studies [20, 21]: Changes < 10% were interpreted as unchanged, 10%–20% as slight improvements or deteriorations, and > 20% as significant improvements or deteriorations in water quality.

2.3.4 | OPI

The OPI is a synthetic indicator used to characterize the degree of organic contamination in aquatic environments. In this study, the OPI was determined following the procedure described in Refs. [10, 11], using parameters such as ammonium (NH_4^+), BOD_5, and nitrite (NO_2^-) together with orthophosphate (PO_4^{3-}). Each parameter was assigned a class value according to predefined concentration ranges, with five possible classes representing increasing levels of organic pollution. The class limits and interpretation criteria are presented in Tables 3 and 4.

2.3.5 | TLI

The trophic status of the lake was determined based on the TLI proposed by Ref. [22]. The index is an integrated measure of lake eutrophication based on four variables, namely, Secchi depth (SD, m) as a measure of water transparency; chlorophyll a concentration (Chl a, mg m^{-3}) as a proxy for phytoplankton biomass; total phosphorus (TP, mg m^{-3}) as an indicator of nutrient enrichment; and total nitrogen (TN, mg m^{-3}) as an indicator of nitrogen availability. Each parameter was transformed into a trophic level score, using the logarithmic equations defined by [22]

$$\mathrm{TLI}_{\mathrm{chla}} = 2.22 + 2.54.\mathrm{Log}(\mathrm{chla}), \tag{7}$$

$$\mathrm{TLI}_{\mathrm{SD}} = 5.10 + 2.27 \cdot \mathrm{Log}\left(\frac{1}{\mathrm{SD}} - \frac{1}{40}\right), \tag{8}$$

TABLE 1 | Water pollution index (WPI) classification used in the present study according to Hossain and Patra [13].

WPI value	Water quality classification
WPI < 0.5	Excellent water
0.50 ≤ WPI < 0.75	Good water
0.75 ≤ WPI ≤ 1.00	Moderately polluted water
WPI > 1	Highly polluted water

$$TLI_{TP} = 0.218 + 2.92.Log(TP), \quad (9)$$

$$TLI_{TN} = -3.61 + 3.01.Log(TN). \quad (10)$$

The final TLI value was calculated as the arithmetic mean of the four individual scores:

$$TLI = \frac{TLI_{chla} + TLI_{SD} + TLI_{TP} + TLI_{TN}}{4}. \quad (11)$$

Burns et al. [22] defined thresholds for each parameter so as to classify the trophic state (Table 5). These boundaries serve as a standardized framework for classifying lakes along a continuum ranging from ultramicrotrophic systems, with very low nutrient concentrations and very high water clarity, to hypertrophic systems, with excessive nutrient enrichment, high algal biomass, and severely degraded water quality.

2.3.6 | Nutrient Limitation Type (TN:TP)

The molar ratio of TN: TP based on the framework of [23] was used to evaluate the potential nutrient limitation of the studied lake. They emphasized that the TN:TP ratio is a useful diagnostic to identify the nutrient most likely to be limiting phytoplankton growth. In particular, a ratio < 20 means nitrogen limitation, a ratio > 50 means phosphorus limitation, and intermediate values (20–50) mean a transitional range where limitation may switch between nitrogen and phosphorus depending on local conditions (Table 6). In the present study, this classification was utilized to identify the dominant nutrient limitation regime in the lake ecosystem, which supplemented the trophic state assessment derived from the TLI.

2.4 | Statistical Analysis

A multivariate approach based on principal component analysis (PCA) was used to synthesize the physicochemical and biological dataset, to identify the dominant environmental gradients and to reveal groups of parameters with similar behavior, which may reflect common sources or shared controlling mechanisms.

TABLE 2 | Classification of water quality based on the Nemerow pollution index (NPI).

NPI range	Water quality category	Classification
NPI ≤ 0.7	Excellent quality	I
0.7 < NPI ≤ 1.0	Good quality	II
1.0 < NPI ≤ 2.0	Slightly polluted	III
2.0 < NPI ≤ 3.0	Moderately polluted	IV
NPI > 3.0	Heavily polluted	V

Because only one value was available for each station and season, differences were tested with the Friedman test, which is the nonparametric equivalent of a two-way analysis of variance without replication. Each variable was tested twice. The four seasons were treated as groups and the stations as blocks for the seasonal effect. The three stations were treated as groups and the seasons as blocks for the spatial effect. For analyzing relationships between variables, Spearman's rank correlation coefficient ($n = 12$) was preferred to Pearson's coefficient because of the small sample size and the non-normal distribution of several variables. Significant results were considered at $p < 0.05$. Statistical analyzes were performed in R (Version 4.5.1) [24].

3 | Results

3.1 | Assessment of Physicochemical Variables

The physical parameters of the studied waters showed significant seasonal differences among the three sampling stations (HMZ1, HMZ2, and HMZ3). Water temperature ranged from 10.2°C to 25.9°C was lower in winter and higher in summer and directly affected DO solubility (Figure 2). The turbidity ranged from 4.1 to 30.8 NTU, with peaks in winter and autumn caused by runoff inputs and sediment resuspension, and decreased from HMZ1 toward HMZ3. SD ranged from 49 to 707 cm, with lower values at HMZ1 correlating with higher turbidity, while TSS ranged from 17 to 194 mg/L, apart from an isolated value of 986 mg/L at HMZ2 in autumn. EC averaged about 864 μS/cm (793–965 μS/cm), with the highest value at HMZ1 in winter. The TDS (771–803 mg/L in winter–spring) increased to 2159–2421 mg/L in summer–autumn, as did salinity (from 0.40 to 0.42 to 1.12–1.25 psu), confirming the medium to high degree of mineralization characteristic of hard waters, as also supported by the TH values (226–452 mg/L $CaCO_3$, reaching 1037 mg/L $CaCO_3$ in summer). From a hydrochemical point of view, the pH values were alkaline (8.0–8.6) and within the range suitable for aquatic life, slightly exceeding 8.5 only at HMZ2 in autumn. Cl^- concentrations were in the range of 80–121 mg/L, relatively higher in spring and lower in summer at HMZ2, indicating that chloride did not follow the evaporative trend. The concentrations of SO_4^{2-} ranged from 130 to 199 mg/L in winter–spring and increased to 347–493 mg/L in summer, exceeding the limit of 400 mg/L at HMZ1 and HMZ3, suggesting a seasonal mineral enrichment. Oxygen saturation values ranged between 49% and 102%, with maxima in spring at HMZ2 and HMZ3, caused by higher photosynthetic activity and efficient water aeration, and minima in summer at HMZ1. In terms of nutrient dynamics, NO_3^- concentrations were low in winter–spring (1.4–3.2 mg/L) but increased markedly in summer and autumn (6.3–29.5 mg/L), with the highest levels at HMZ2, likely due to soil leaching and mineralization of organic matter. Concentrations of NO2 − were low (0.01–0.16 mg/L), increasing from spring to autumn with a maximum at HMZ1. NH 4 + was found to be low to moderate (0.08–0.42 mg/L), and higher concentrations were found at all stations in summer, indicating enhanced ammonification of organic matter. PO_4^{3-} levels were low in winter–spring (0.02–0.09 mg/L), but their summer and autumn increase at HMZ1 (0.29 and 0.62 mg/L) identifies the upstream inflow as the main phosphorus input. The organic parameters indicated moderate loads of biodegradable organic matter. BOD_5 ranged from 7.1 to 28.1 mg/L, with low values in winter–spring and a near threefold

TABLE 3 | Classification ranges for pollutant levels.

Parameters classes	BOD_5 (mg · L^{-1})	NH_4^+ (mg · L^{-1})	NO_2^- (μg · L^{-1})	PO_4^{3-} (μg · L^{-1})
5	< 2	< 0.1	< 5	< 15
4	2–5	0.1–0.9	6–10	16–75
3	5.1–10	1–2.4	11–50	76–250
2	10.1–15	2.5–6	51–150	251–900
1	> 15	> 6	> 150	> 900

increase at all stations during summer–autumn, indicating seasonal organic inputs. COD values ranged from 8.9 to 35.1 mg/L, with a COD/BOD_5 ratio of about 1.25, reflecting the predominance of biodegradable organic compounds. Primary production, estimated via Chl a, was moderate (2.1–12.4 μg/L), with distinct spring peaks (up to 12.4 μg/L at HMZ3) and a summer peak at HMZ1 (11.3 μg/L), suggesting algal growth driven by nutrient availability and favorable photic conditions. Conversely, lower concentrations in autumn (3.4–4.3 μg/L) and in summer at HMZ2 (≈2 μg/L) were caused by seasonal decreases in phytoplankton activity.

3.2 | WPI

WPI values computed from the eleven parameters ranged from 0.60 to 1.27 (Figure 3; Table S1) and showed a clear seasonal pattern combined with a consistent upstream-to-dam gradient. In winter, all three stations fell in the moderate pollution class (0.75–1), with values decreasing from the upstream station HMZ1 (0.98) to the mid-reservoir station HMZ2 (0.93) and the embankment station HMZ3 (0.80). Spring recorded the lowest values of the year: HMZ2 (0.65) and HMZ3 (0.60) were classified as good (0.5–0.75), whereas HMZ1 remained moderately polluted (0.87). In summer, the index exceeded the threshold of 1 at all stations (HMZ1: 1.19; HMZ2: 1.02; HMZ3: 1.02), and autumn showed the highest values of the annual cycle (HMZ1: 1.27; HMZ2: 1.19; HMZ3: 1.06), placing the whole reservoir in the highly polluted class. The seasonal mean WPI thus decreased from 0.90 in winter to 0.71 in spring, before rising to 1.08 in summer and 1.17 in autumn. Of the 12 seasonal observations, 50% were classified as highly polluted, 33% as moderately polluted, and 17% as good; none reached the excellent class.

Spatially, HMZ1 recorded the highest WPI in every season (annual mean 1.08), followed by HMZ2 (0.95) and HMZ3 (0.87). The contrast between stations was most pronounced in winter and spring (up to 0.27 WPI units in spring) and weakened in summer (≤ 0.17 units), indicating more uniform conditions across the reservoir during the warm season.

TABLE 4 | Classification of organic pollution status based on OPI.

Organic pollution value	Organic pollution classes
5–4.6	No organic pollution
4.5–4	Low organic pollution
3.9–3	Moderate organic pollution
2.9–2	High organic pollution
1.9–1	Very high organic pollution

The pollution loads of the individual parameters (Figure 3; Table S1) show that the WPI was controlled by a small number of variables. Throughout winter and spring, nine of the eleven parameters had PL values below 1, and only turbidity (PL = 1.67–6.16) and TDS (PL = 1.54–1.63) exceeded their permissible limits. Turbidity was the dominant contributor during the wet season, particularly upstream (PL = 6.16 at HMZ1 in winter). In summer, the dominant contributors shifted to TDS (PL = 4.66–4.84), total hardness (PL = 2.05–2.07), and sulfate (PL up to 1.23 at HMZ3). In autumn, TDS and turbidity were again the main contributors (PL = 3.56–4.73), together with orthophosphate at HMZ1 (PL = 1.24) and pH at HMZ2 (PL = 1.04). Nitrate, nitrite, ammonium, and chloride remained well below their limits at all stations and in all seasons (PL ≤ 0.59).

3.3 | NPI

The outcomes of the water quality assessment based on the NPI are shown in Figure 4. The NPI was computed from the same eleven parameters used for the WPI (pH, NH_4^+, NO_2^-, NO_3^-, PO_4^{3-}, SO_4^{2-}, Cl^-, TH, EC, TDS, and turbidity) and the corresponding World Health Organization (WHO) (2011) standards. The single-factor indices (P_i) of all parameters and the parameter responsible for Pmax in each sample are given in Figure S1. For the Hamiz reservoir, the NPI values ranged from 1.25 to 4.41, where higher scores indicate a decline in water quality. Over the study period, the monitoring stations were classified between Cases III and V (Table 2), with 83% of the samples (10 of 12) in Class V. During winter, the NPI values ranged from 3.15 to 4.41 at all stations (HMZ1, HMZ2, and HMZ3), placing the reservoir in Class V (heavily polluted). The highest value of the annual cycle was recorded at HMZ1 (4.41), and values decreased toward the dam (HMZ2: 4.12; HMZ3: 3.15). In spring, the NPI decreased markedly at HMZ2 (1.53) and HMZ3 (1.25), placing them in Class III (slightly polluted), whereas HMZ1 remained in Class V (3.30). During summer (3.37–3.52) and autumn (3.14–3.46), all stations were again in Class V, with narrow differences between stations.

The analysis of Pmax showed that the NPI was controlled by only two parameters (Figure 4. S1). In winter and spring, Pmax was always associated with turbidity (P_i = 1.67–6.16), the highest values being recorded at HMZ1 (6.16 in winter; 4.59 in spring), reflecting the input of suspended particles by runoff during the wet season. In summer, Pmax shifted to TDS at all stations (P_i = 4.66–4.84), together with high P_i values of TH (2.05–2.07) and SO_4^{2-} (up to 1.23), indicating the increase in mineralization during the dry season. In autumn, Pmax was associated with TDS at HMZ1 (4.73) and HMZ3 (4.32) and with turbidity at HMZ2 (4.72). Both parameters exceeded their standards about fourfold at all stations, reflecting the combined effect of dry-season

TABLE 5 | Values of variables that define the boundaries of different trophic levels ([22]).

Lake type	Trophic level (TLI)	Chlorophyll a (mg m^{-3})	Secchi depth (m)	Total phosphorus (mg P m^{-3})	Total nitrogen (mg N m^{-3})
Ultra-microtrophic	0.0–1.0	0.13–0.33	33–25	0.84–1.8	16–34
Microtrophic	1.0–2.0	0.33–0.82	25–15	1.8–4.1	34–73
Oligotrophic	2.0–3.0	0.82–2.0	15–7.0	4.1–9.0	73–157
Mesotrophic	3.0–4.0	2.0–5.0	7.0–2.8	9.0–20	157–337
Eutrophic	4.0–5.0	5.0–12	2.8–1.1	20–43	337–725
Supertrophic	5.0–6.0	12–31	1.1–0.4	43–96	725–1558
Hypertrophic	6.0–7.0	> 31	< 0.4	> 96	> 1558

mineralization and the first autumn runoff events. In contrast, nutrients (NH_4^+, NO_2^-, NO_3^-) and Cl^- never controlled the NPI ($P_i \leq 0.59$), and PO_4^{3-} exceeded its standard only at HMZ1 in autumn ($P_i = 1.24$).

Compared with the WPI, the NPI provided a more severe classification, particularly in winter. The WPI then indicated moderate pollution (0.80–0.98), whereas the NPI classified all stations as heavily polluted. This difference results from the structure of the Nemerow index, which gives greater weight to the most polluting parameter. A single parameter exceeding its standard several-fold (turbidity in winter) is enough to classify the water as heavily polluted, even when the average pollution load (Pavg = 0.80–0.98) remains below 1. = 0.80–0.98) remains below 1.

3.4 | Water Quality Variability Across Space and Time in the Hamiz Reservoir

The spatiotemporal analysis of the NPI for the El Hamiz reservoir revealed marked variations in both time and space (Table 7). Positive change rates indicate an improvement in water quality and negative rates a deterioration.

The temporal change rate (T%) showed that water quality varied considerably from one season to the next. The transition from winter to spring brought a significant improvement (+47.94%), the mean NPI falling from 3.89 to 2.03. This improvement is mainly related to the decrease in turbidity once the winter runoff events ended, particularly at HMZ2 and HMZ3. It was followed by the sharpest change in the annual cycle, a severe deterioration from spring to summer (−69.07%), during which the mean NPI rose to 3.43. This degradation coincides with the dry season, when high temperatures and evaporation increase the mineral content of the water, TDS becoming the parameter with the highest pollution index at all stations. Between summer and autumn, the NPI hardly changed (+2.30%, < 10%), as the effect of mineralization persisted while turbidity rose again with the first autumn rains. Finally, the transition from autumn to winter showed a moderate deterioration (−16.29%), the mean NPI reaching its annual maximum in winter (3.89) under the influence of high turbidity linked to runoff and sediment inputs. The temporal analysis therefore shows that the reservoir does not recover during the wet season, as might be expected. Spring is the most favorable period for water quality, whereas winter and summer are the most critical, for different reasons: particulate inputs in winter, mineralization in summer.

The spatial change rate (S%), calculated between the upstream station HMZ1 and the embankment station HMZ3, showed a strong seasonal contrast. In winter and spring, water quality was clearly heterogeneous across the reservoir, with spatial change rates of 28.50% and 62.11%, respectively. In both seasons, the NPI decreased from HMZ1 toward the dam, and in spring, HMZ1 remained heavily polluted (3.30), while HMZ3 was only slightly polluted (1.25). This gradient reflects the role of the upstream zone as the main entry point of turbid runoff water, the suspended particles then settling progressively along the reservoir. In summer and autumn, by contrast, the spatial variability was low (4.29% and 9.29%), below the 10% threshold, indicating that the three stations were affected in a similar way. During this period, the deterioration of water quality was controlled by processes acting at the scale of the whole water body, mainly the evaporative concentration of dissolved salts, rather than by local inputs. Overall, the El Hamiz reservoir behaves as a spatially heterogeneous system during the wet season and becomes almost uniform during the dry season, when pollution levels are high throughout.

3.5 | OPI

The OPI showed a clear contrast between the cool and the warm halves of the year, with half of the observations in the moderate organic pollution class and the other half in the high organic pollution class (Figure 5, Table S2). In winter, the three stations fell in the moderate class, with values of 3.50 at HMZ1 and HMZ3 and 3.75 at HMZ2. Spring values were very similar (3.25–3.75), the lowest being recorded at the mid-reservoir station HMZ2 and the highest at the embankment station HMZ3. In both seasons,

TABLE 6 | Thresholds of TN:TP molar ratio for nutrient limitation type (Guildford and Hecky [23]).

TN:TP molar ratio	Nutrient limitation type	Ecological interpretation
< 20	Nitrogen limitation	Phytoplankton growth likely limited by nitrogen availability
20–50	Transitional zone	Limitation can shift between nitrogen and phosphorus depending on conditions
> 50	Phosphorus limitation	Phytoplankton growth likely limited by phosphorus availability

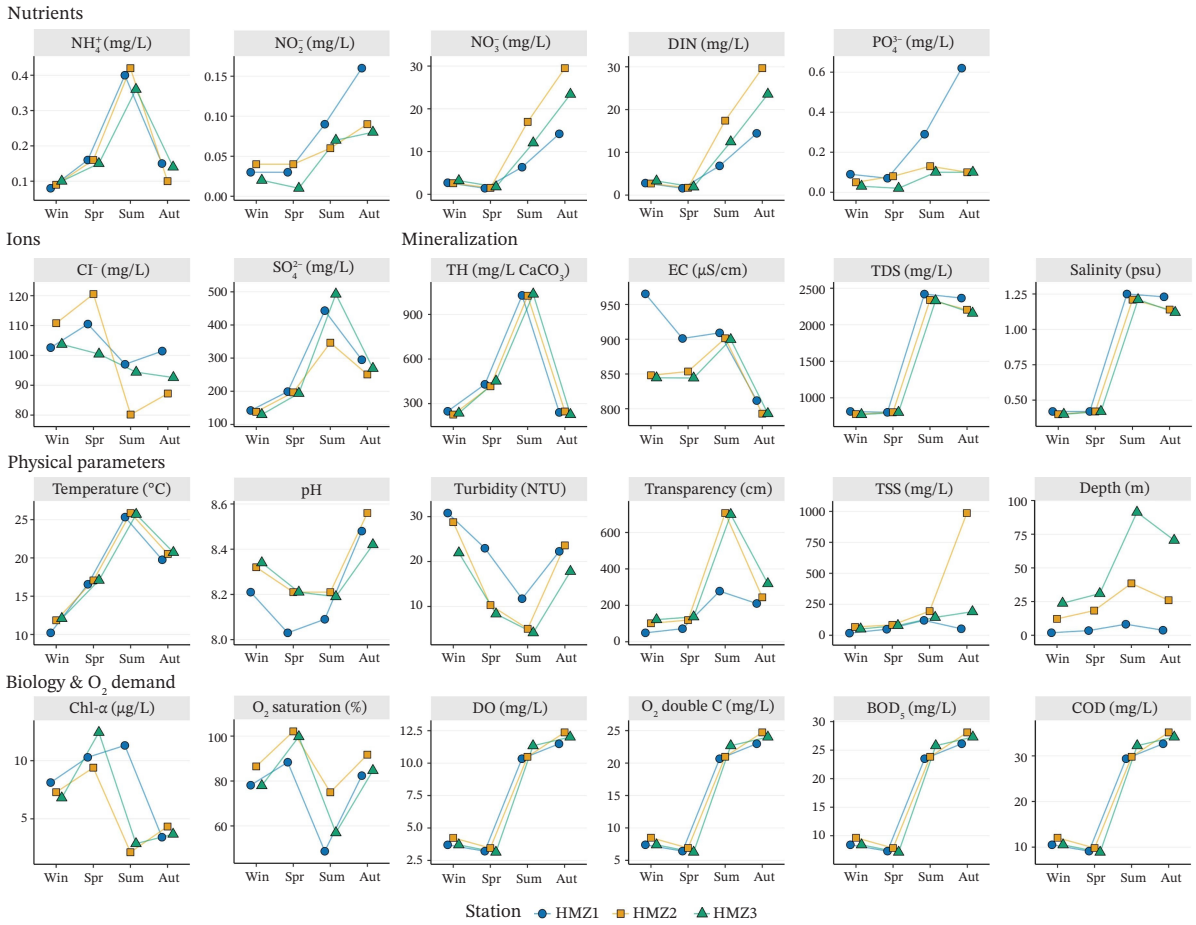

FIGURE 2 | Seasonal variation in physicochemical and biological variables at the three sampling stations of the El Hamiz reservoir (2018).

BOD_5 (7.1–9.7 mg/L) and nitrite (10–40 µg/L) obtained intermediate scores, while ammonium remained low (0.08–0.16 mg/L) and contributed little to the organic load. In summer, the index dropped to 2.25 at HMZ1 and 2.50 at HMZ2 and HMZ3, placing the whole reservoir in the high organic pollution class. The situation was similar in autumn, when HMZ2 and HMZ3 kept a value of 2.50 and HMZ1 reached 2.00, the lowest value of the annual cycle, at the limit of the very high organic pollution class. This warm-season deterioration was mainly driven by BOD_5, which exceeded 15 mg/L at all stations (23.5–28.1 mg/L) and therefore obtained the lowest possible score, together with the increase in nitrite (60–160 µg/L) and, at HMZ1, in orthophosphate (290–620 µg/L). Spatially, the differences between stations were small in every season, not exceeding 0.5 units. However, HMZ1 recorded the lowest OPI in summer and autumn, which points to a greater organic and nutrient input near the inflow. The seasonal shift from moderate to high organic pollution was observed simultaneously at the three stations. This suggests that the organic load of the reservoir is governed mainly by processes acting at the scale of the whole water body during the warm season, such as the decomposition of organic matter at higher temperature and reduced water renewal, with an additional contribution of local inputs in the upstream zone.

3.6 | TLI

The trophic status of the El Hamiz reservoir, assessed with the TLI, remained high throughout the year, with values between 4.65 and 5.94 (Figure 6). The reservoir was therefore eutrophic to supertrophic in all seasons. Two-thirds of the observations fell in the supertrophic class and the remaining third in the eutrophic class, while none of them reached the hypertrophic threshold of 6. In winter, TLI values ranged from 4.83 to 5.40; the upstream station HMZ1 was already supertrophic at the beginning of the hydrological cycle, whereas HMZ2 and HMZ3 were eutrophic. Spring brought a slight decrease (4.65–5.11), probably due to dilution by seasonal inflows, but HMZ1 and HMZ2 stayed in the supertrophic range. Values rose again in summer (4.93–5.71), in line with higher temperatures and reduced water renewal, and the most critical conditions were observed in autumn, when the three stations were all supertrophic and the TLI reached 5.43 to 5.94. On a seasonal basis, the mean TLI was lowest in spring (4.93), followed by winter (5.07) and summer (5.23), and highest in autumn (5.66). Spatially, the index decreased from the inflow toward the dam in every season, with annual means of 5.54 at HMZ1, 5.17 at HMZ2 and 4.96 at HMZ3, and the difference between stations within a given season never exceeded 0.8 units. Enrichment therefore concerns the whole water body, but it is more pronounced near the inflow.

3.7 | Nutrient Limitation Type (TN:TP)

NPL reveals a persistent shoreline transitional zone and dominant phosphorus limitation in pelagic and embankment waters, punctuated by a brief spring nitrogen-limited window mid-reservoir. Upstream at HMZ-1, nutrient stoichiometry remains

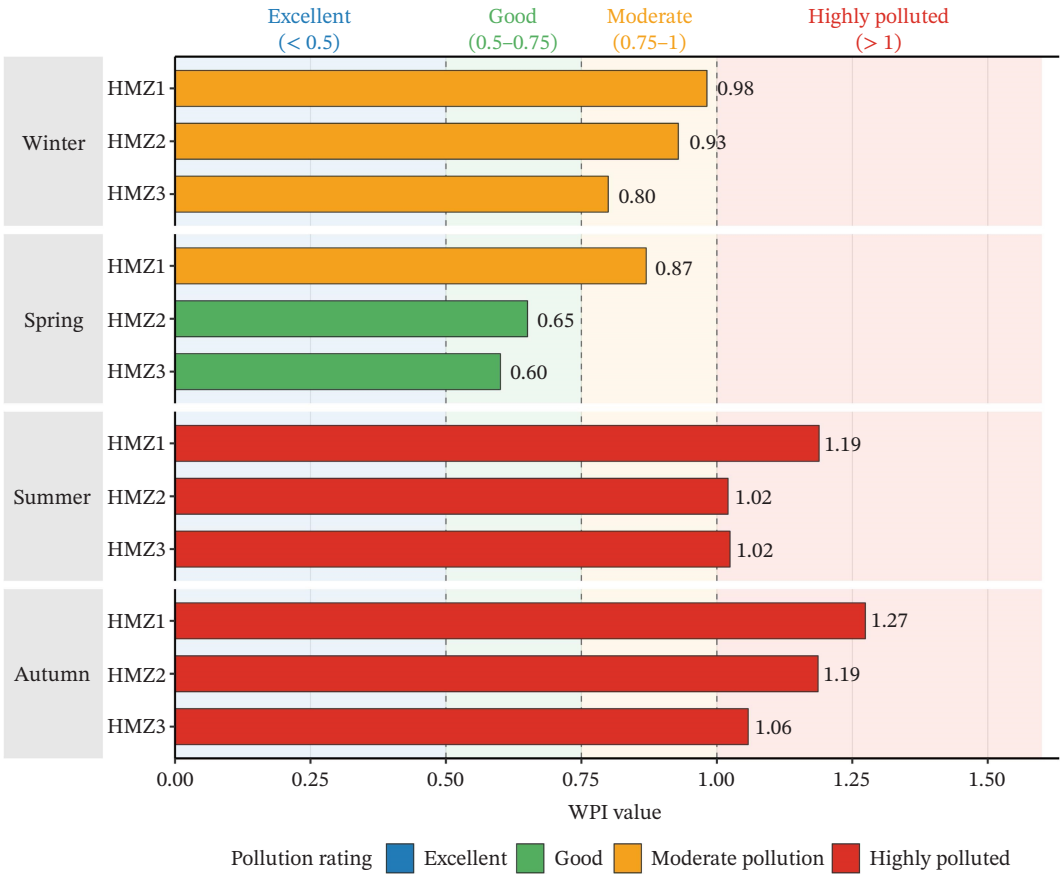

FIGURE 3 | Seasonal water pollution index (WPI) at the three sampling stations of the El Hamiz reservoir (2018).

in the transitional zone throughout the year: winter (28.78), spring (20.14), summer (22.18), and autumn (22.88), matching the (20–50) reference interval for transitional conditions (Figure 7). This persistent transitional status suggests a variable N/P balance near the shore, likely shaped by episodic inputs, rapid sediment-water exchanges, and localized uptake. At the mid-reservoir HMZ-2, winter (51.53) already indicates phosphorus limitation (> 50), followed by a distinct nitrogen limitation episode in spring (19.39; < 20), and then, a strong return to phosphorus limitation in summer and autumn (132.09 and 309.63). At the embankment HMZ-3, all seasons are phosphorus limited (104.62 in winter; 71.29 in spring; 119.55 in summer; and 243.60 in autumn), signaling a robust pelagic near-dam regime in which phosphorus is the primary constraint on algal production. Spatially, the system comprises a shoreline transitional pocket (HMZ-1) against P-limited open water (HMZ-2 and HMZ-3), with a short spring N-limited window in the mid-reservoir. Seasonally, phosphorus limitation strengthens from spring to autumn in the pelagic and embankment zones, consistent with stratification, particulate settling, and internal processing that reinforce P scarcity relative to N in the open water.

3.8 | Statistical Analysis

The PCA was carried out on eighteen standardized variables (correlation matrix) measured at three stations over four seasons ($n = 12$). Variables obtained by calculation from other measurements (COD and the two oxygen variables derived from BOD_5) and the sum of the inorganic nitrogen forms (DIN) were excluded in order to avoid giving artificial weight to the same information. Four components had eigenvalues greater than 1 (9.11, 4.53, 1.76, and 1.02), but the scree plot shows a clear break after the third. The first two components accounted for 75.8% of the total variance (PC1: 50.6%; PC2: 25.2%) and the first three for 85.6%. The factorial plane PC1–PC2 therefore summarizes most of the information, while PC3 (9.8%) adds a smaller but interpretable signal. Most variables were well represented on the first plane, with squared cosines above 0.9 for BOD_5, TDS, salinity, total hardness, ammonium, pH, sulfate, and temperature. Orthophosphate (0.25) and TSS (0.46) were poorly represented on this plane, and their behavior is better described by PC3 (Figure 8).

PC1 is the main gradient of the dataset and has a clear seasonal meaning. On its positive side, it gathers the variables of mineralization, salinity and TDS (loadings of 0.98), sulfate (0.89), and total hardness (0.65); the organic load, with BOD_5 (0.93); the inorganic nitrogen forms, ammonium (0.74), nitrate (0.71), and nitrite (0.69); and together with temperature (0.92) and transparency (0.85). On its negative side, it gathers chloride (−0.77), chlorophyll a (−0.64), oxygen saturation (−0.60), and turbidity (−0.54). The variables that contributed most to this axis were TDS and salinity (10.5% each), BOD_5 (9.6%), temperature (9.3%), sulfate (8.8%), and transparency (7.9%) (Figure S2).

This axis therefore describes the passage from wet-season to dry-season conditions. In the wet season, the water is cooler, more turbid, and better oxygenated, with relatively more chloride and a higher algal biomass. In the dry season, the water warms up and becomes clearer, while dissolved salts, organic matter, and

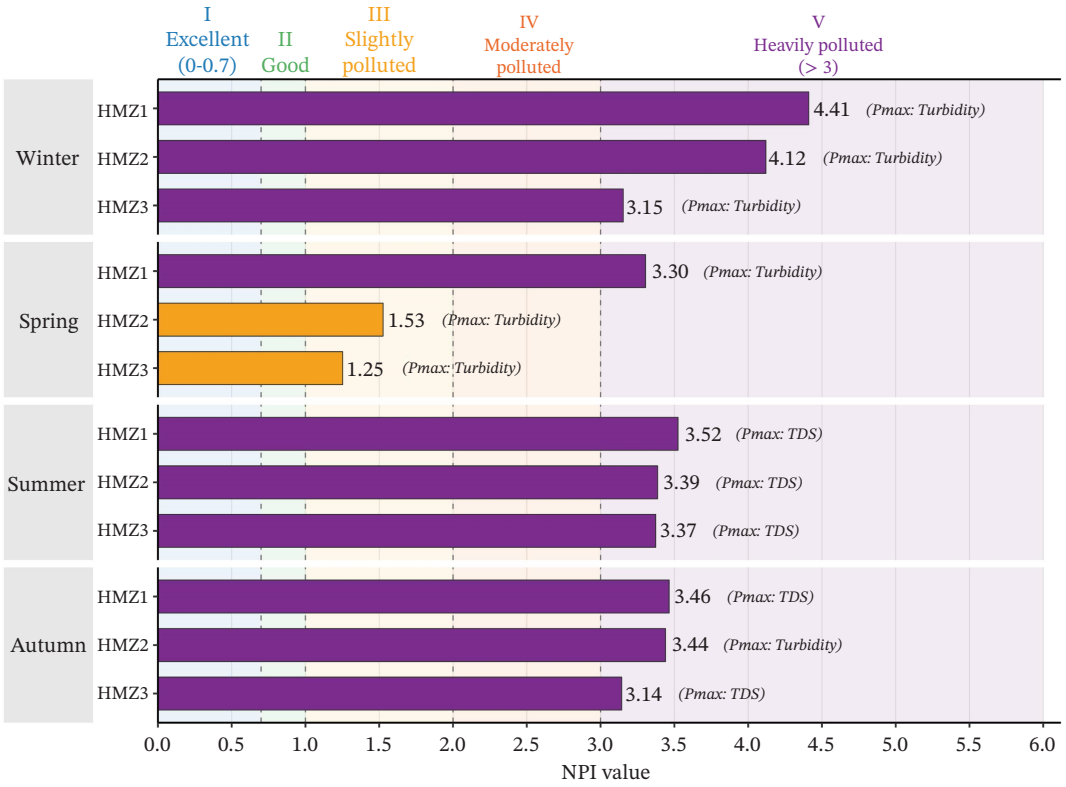

(a)

	pH	NH_4^+	NO_2^-	NO_3^-	PO_4^{3-}	SO_4^{2-}	Cl^-	TH	EC	TDS	Turbidity	P_{avg}	P_{max}
Winter - HMZ1	0.81	0.05	0.01	0.05	0.18	0.35	0.41	0.50	0.64	1.63	6.16	0.98	6.16
Winter - HMZ2	0.88	0.06	0.01	0.05	0.10	0.34	0.44	0.45	0.57	1.55	5.75	0.93	5.75
Winter - HMZ3	0.89	0.07	0.01	0.06	0.06	0.32	0.41	0.47	0.56	1.54	4.39	0.80	4.39
Spring - HMZ1	0.69	0.11	0.01	0.03	0.14	0.50	0.44	0.86	0.60	1.60	4.59	0.87	4.59
Spring - HMZ2	0.81	0.11	0.01	0.03	0.16	0.49	0.48	0.83	0.57	1.61	2.06	0.65	2.06
Spring - HMZ3	0.81	0.10	< 0.01	0.03	0.04	0.48	0.40	0.90	0.56	1.60	1.67	0.60	1.67
Summer - HMZ1	0.73	0.27	0.03	0.13	0.58	1.11	0.39	2.06	0.61	4.84	2.35	1.19	4.84
Summer - HMZ2	0.81	0.28	0.02	0.34	0.26	0.87	0.32	2.05	0.60	4.68	1.00	1.02	4.68
Summer - HMZ3	0.79	0.24	0.02	0.24	0.20	1.23	0.38	2.07	0.60	4.66	0.83	1.02	4.66
Autumn - HMZ1	0.99	0.10	0.05	0.28	1.24	0.74	0.41	0.48	0.54	4.73	4.45	1.27	4.73
Autumn - HMZ2	1.04	0.07	0.03	0.59	0.20	0.63	0.35	0.49	0.53	4.41	4.72	1.19	4.72
Autumn - HMZ3	0.95	0.09	0.03	0.47	0.20	0.67	0.37	0.45	0.53	4.32	3.56	1.06	4.32

$P_i = C_i/S_i$: 4, 2, 1, 0.5, 0.1, 0.01

NPI = sqrt((Pavg² + Pmax²)/2). Black frame = parameter giving Pmax in each sample; Pi > 1 = WHO (2011) standard exceeded.

(b)

FIGURE 4 | (a) Seasonal Nemerow pollution index (NPI) at the three sampling stations of the El Hamiz reservoir (2018); the parameter responsible for P_{max} is indicated for each sample. (b) Seasonal organic pollution index (OPI) at the three sampling stations of the El Hamiz reservoir (2018).

nitrogen accumulate. Two features of this axis deserve attention. First, chloride lies on the opposite side from TDS and salinity, whereas sulfate lies on the same side. The summer increase in mineralization is therefore carried by sulfate rather than by chloride, which agrees with the Spearman correlations and points to the dissolution of sulfate-bearing formations and to agricultural inputs, in addition to evaporation. Second, chlorophyll a is opposed to BOD_5 and nitrate. The highest algal biomass did not coincide with the period of maximum enrichment, which is consistent with the spring peaks of chlorophyll a and with the

TABLE 7 | Spatial-temporal variation rate of the Hamiz reservoir.

Variation	Transition/season	Gt_1/Gs_1	Gt_2/Gs_2	Change rate (%)	Magnitude category (%)	Interpretation
Temporal (T%)	Winter–spring	3.89	2.03	**+47.94**	> 20	Significant improvement
	Spring–summer	2.03	3.43	**−69.07**	> 20	Significant deterioration
	Summer–autumn	3.43	3.35	**+2.30**	< 10	Essentially unchanged (slight improvement)
	Autumn–winter	3.35	3.89	**−16.29**	10–20	Moderate deterioration
Spatial (S%)	Winter	4.41	3.15	**+28.50**	> 20	Marked spatial heterogeneity
	Spring	3.30	1.25	**+62.11**	> 20	Marked spatial heterogeneity
	Summer	3.52	3.37	**+4.29**	< 10	Homogeneous water quality
	Autumn	3.46	3.14	**+9.29**	< 10	Homogeneous water quality

Note: The bold positive values indicate an improvement in water quality, and the negative ones show a deterioration in water quality with percentage.

lower values recorded in summer and autumn. The position of transparency on the positive side of PC1 also confirms that the water was clearer in the warm season, after the runoff period had ended.

PC2 is mainly defined by pH (0.94), which alone accounts for 19.5% of the axis, together with nitrate (0.62), TSS (0.58), turbidity (0.54), and oxygen saturation (0.47) on the positive side. On the negative side, it is defined by EC (−0.79), total hardness (−0.74), and ammonium (−0.65) and to a lesser extent by chlorophyll a (−0.43) and sulfate (−0.36). This axis does not separate the wet season from the dry season; it separates the two-halves of the dry season from each other.

Summer samples lie on the negative side of PC2, in the direction of hardness, ammonium, and EC. This combination indicates warm, slowly renewed water in which dissolved salts accumulate and organic matter decomposes, releasing ammonium. Autumn samples lie on the positive side, with higher pH, nitrate, TSS, and turbidity. The shift from ammonium in summer to nitrate in autumn is consistent with the nitrification of the ammonium accumulated during the warm months, while the higher TSS and turbidity reflect the first autumn runoff events. The higher pH in autumn may be related to these changes in the carbonate balance and to the inputs of runoff water from the calcareous catchment. PC2 thus shows that summer and autumn, although both belonging to the degraded period, are governed by different processes: accumulation and decomposition in summer, nitrification, and renewed particulate inputs in autumn (Figure S2).

PC3 is dominated by orthophosphate (loading 0.81; 37.6% of the axis) and nitrite (0.56; 17.6%), with TSS on the negative side (−0.47; 12.7%). The sample contributing most to this axis is HMZ1 in autumn (50.4% of the axis), followed by HMZ2 in autumn and HMZ1 in summer. This component therefore isolates the orthophosphate and nitrite peaks recorded at the upstream station during the warm season. It shows that phosphorus inputs do not follow the general seasonal pattern described by PC1, but are concentrated near the inflow. This explains why orthophosphate was poorly represented on the first plane and why it showed no significant seasonal effect in the Friedman test.

The projection of the samples on the PC1–PC2 plane shows three well-separated groups. Winter and spring samples form a single group on the negative side of PC1 (scores from −3.3 to −2.6), which indicates that the two wet-season periods are similar in terms of overall water chemistry. Within this group, winter samples lie slightly higher on PC2 than spring samples, in the direction of turbidity and oxygen saturation, in agreement with the higher winter turbidity. Summer samples lie on the positive side of PC1 and the negative side of PC2 (PC1 from 3.1 to 4.3; PC2 from −2.9 to −1.7), and they contribute most to PC1. Autumn samples lie on the positive side of both axes and dominate PC2, HMZ2 in autumn alone accounting for 34.7% of this axis (Figure 8).

Within each season, the three stations remain close to one another, and the distance between seasons is much greater than the distance between stations. This confirms the result of the Friedman test, which detected significant seasonal differences for fourteen variables but spatial differences for only seven. Nevertheless, a spatial pattern can be seen within the seasons. In

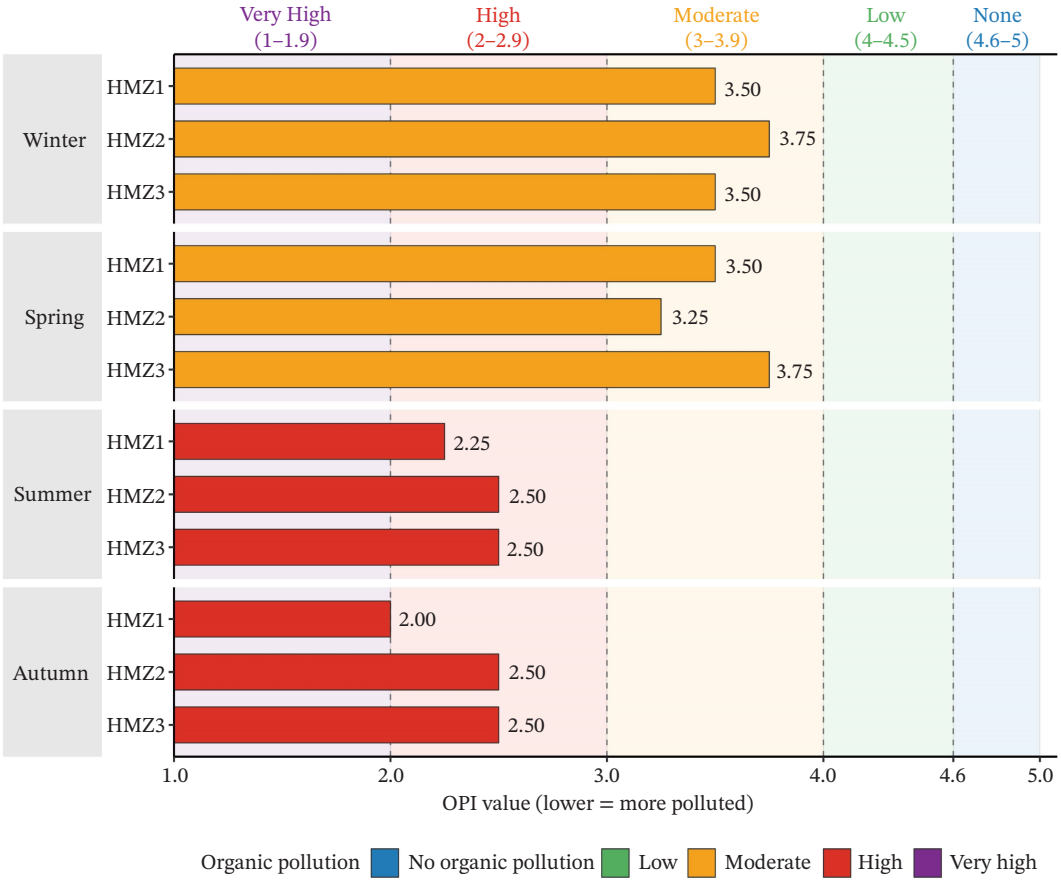

FIGURE 5 | Seasonal dynamics of the pollution index in the El Hamiz reservoir.

winter and spring, HMZ1 lies furthest from the other stations, on the side of higher turbidity and lower transparency, which is consistent with the upstream-to-dam gradient shown by the spatial change rate of the NPI. In summer and autumn, HMZ1 is mainly separated along PC3 because of its phosphorus and nitrite inputs (Figures S2, S3).

The PCA helps to understand the behavior of the indices. The two parameters that controlled Pmax in the Nemerow index lie on two different axes: TDS is one of the main variables of PC1 and characterizes the dry season, whereas turbidity lies on the negative side of PC1 and characterizes the wet season. This explains why the NPI remained high in both winter and summer, for different reasons. The OPI is linked to PC1 through BOD_5 and nitrite, which explains the shift from moderate to high organic pollution between the wet and dry seasons. The TLI combines variables located on opposite sides of PC1, chlorophyll a and transparency on the one hand and nutrients on the other, which partly explains why its seasonal variation remained moderate (Figure 8).

4 | Discussion

Surface water quality in artificial reservoirs is governed by a complicated interaction between geogenic processes, climatic constraints, and anthropogenic pressures, the relative contributions of which vary according to season and region [24, 25]. In the Mediterranean context of North Africa, including subhumid areas such as the El Hamiz catchment, these interactions are shaped by the contrast between a wet season, when runoff carries particles and dissolved substances into reservoirs, and a long dry season marked by evaporation, longer water residence time, and intensive agricultural land use, which render single physico-chemical parameters insufficient for a comprehensive diagnosis [26–29]. The multi-index approach was applied to the El Hamiz reservoir, a strategic water resource in the north of Algeria, using the WPI, NPI, OPI, TLI, and TN:TP ratio at three monitoring stations (HMZ1, HMZ2, and HMZ3). This methodology is based on the work of Hossain and Patra [13], Chidiac et al. [30], and Uslu et al. [31]. It offers a multidimensional diagnosis that reveals two critical periods, winter, dominated by particulate inputs, and summer–autumn, dominated by mineralization and organic load, together with persistent eutrophic-to-supertrophic conditions throughout the year.

Water temperature ranged from 10.2°C to 25.9°C, being lower in winter and higher in summer, which is within thermally acceptable limits for aquatic life and directly affected DO solubility. This range is comparable to those of other Algerian reservoirs, like Babar where temperatures ranged from 3.0°C to 20.6°C [32] and 7°C–32°C [27]. Oxygen saturation varied between 49% and 102%, with spring maxima at HMZ2 and HMZ3 due to increased photosynthetic activity and efficient aeration, and summer minima at HMZ1. The summer oxygen depletion is due to the higher BOD and the thermal inhibition of DO solubility that has been described for Mediterranean reservoirs [33, 34]. pH was consistently alkaline (8.0–8.6) and within the WHO (2011) [35] acceptable range of 6.5–8.5 (slightly exceeded only at HMZ2 in

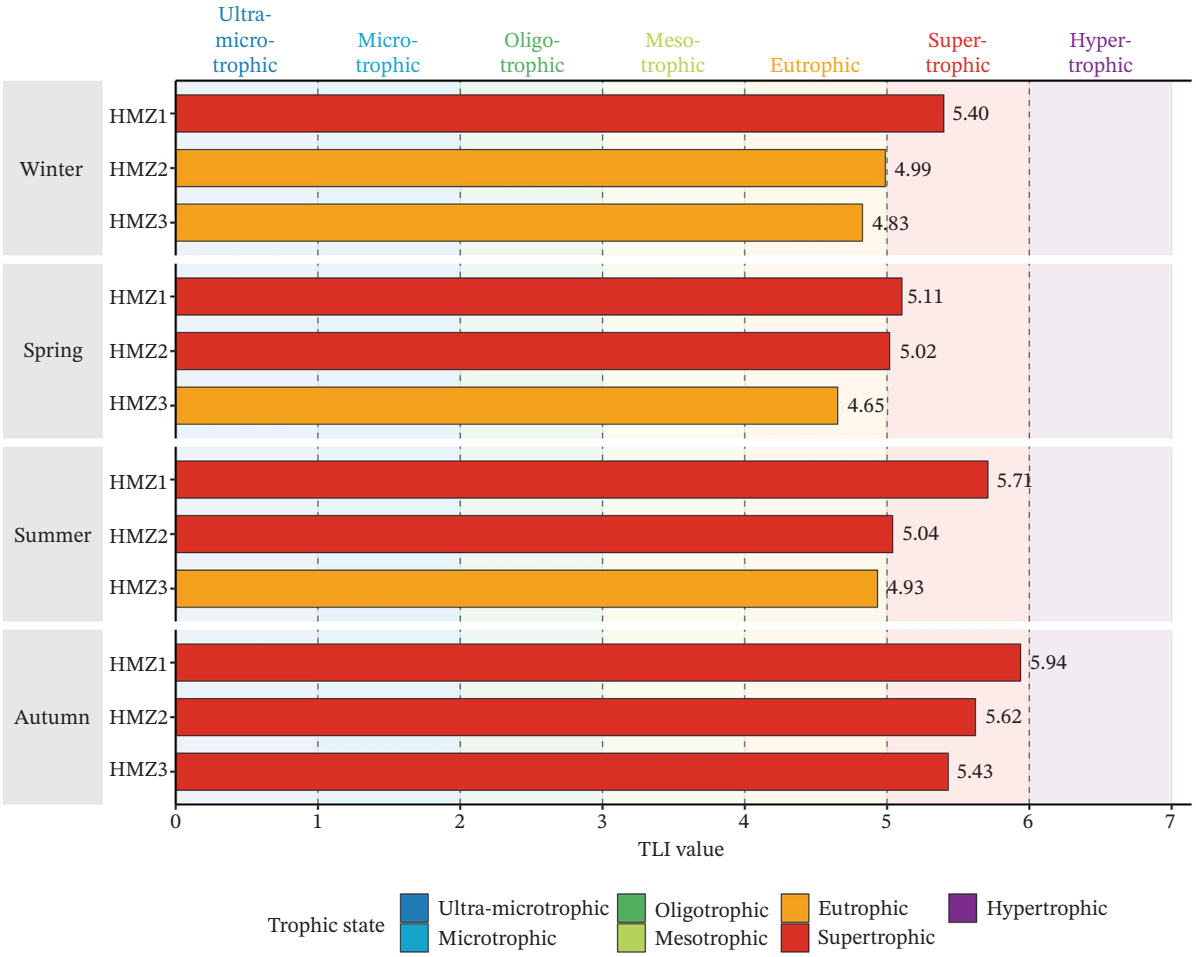

FIGURE 6 | Seasonal trophic level index (TLI) with the trophic classes at the three sampling stations of the El Hamiz reservoir (2018).

autumn), consistent with the carbonate–bicarbonate buffering capacity of the limestone geology of the catchment [34]. These values are comparable to those reported at Babar (7.78 ± 0.175) by Gaagai et al. [27], Koudiat Medouar (7.73–8.3) Bouslah [36] and Bouchema et al. [37], and Beni Haroun Dam [29]. The highest pH values were recorded in autumn and the lowest in spring at HMZ1, where the inflow of runoff water is most direct.

The mineral content of El Hamiz water was moderate in winter–spring and high in summer–autumn. EC averaged ≈ 864 µS/cm (793–965 µS/cm) and remained below its permissible limit throughout the year (PL = 0.53–0.64), whereas TDS exceeded the WHO drinking water threshold of 500 mg/L in all seasons (0% compliance), with 771–803 mg/L in winter–spring and 2159–2421 mg/L in summer–autumn (PL = 1.54–4.84). Mineralization of this kind is common in reservoirs draining evaporitic and carbonate watersheds [38, 39]. Winter–spring TDS at El Hamiz was lower than at Babar (1109.53 ± 72.30 mg/L; EC: 1070–1400 µS/cm) [27, 40] and Ourkiss (1309.92 ± 141.12 mg/L) [40], two reservoirs of the semiarid east of the country, which is consistent with the greater dilution expected under the higher rainfall of the subhumid stage; summer–autumn values, by contrast, were about twice as high. EC was in the lower range of Timgad (848–1534 µS/cm) [37, 40]. The role of geology is illustrated by the lower mineralization of the Yabous Dam (TDS: 532.85 ± 35.41 mg/L) [37]. In the region, the weathering of evaporitic formations (gypsum, halite, and anhydrite) and carbonates is the dominant natural source of dissolved salts [41–43], and urban wastewater, NPK fertilizers, and other anthropogenic outputs add to this load [44, 45]. The summer–autumn increase in TDS, salinity (from 0.40 to 0.42 to 1.12–1.25 psu), and total hardness can be attributed to evaporoconcentration during the 6-month dry season, a process documented in Mediterranean reservoirs during the dry period [46–49]. However, this increase was mainly associated with sulfate ($\rho = 0.90$ and 0.93 with TDS and salinity), whereas chloride did not follow the evaporative trend (lower in summer; ρ with temperature = −0.81). The PCA leads to the same conclusion, since sulfate lies with TDS and salinity on the positive side of PC1, whereas chloride lies on the opposite side. This suggests that, besides evaporation, the dissolution of sulfate-bearing formations and sulfate-based fertilizers contributed to the summer mineral enrichment. The magnitude of this enrichment is nevertheless high for a subhumid reservoir and deserves confirmation by further monitoring. The total hardness (TH: 226–452 mg/L $CaCO_3$, reaching 1037 mg/L $CaCO_3$ in summer) classified the water as hard to very hard, reflecting the Tell Atlas lithology [42, 50].

Chloride concentrations (80–121 mg/L) were below the WHO limits (< 250 mg/L; 100% compliance) (PL ≤ 0.48). In contrast to TDS, chloride did not follow an evaporative trend, with higher values in spring and lower values in summer at HMZ2, which points to a limited contribution of evaporative concentration, although moderate urban effluent inputs cannot be excluded.

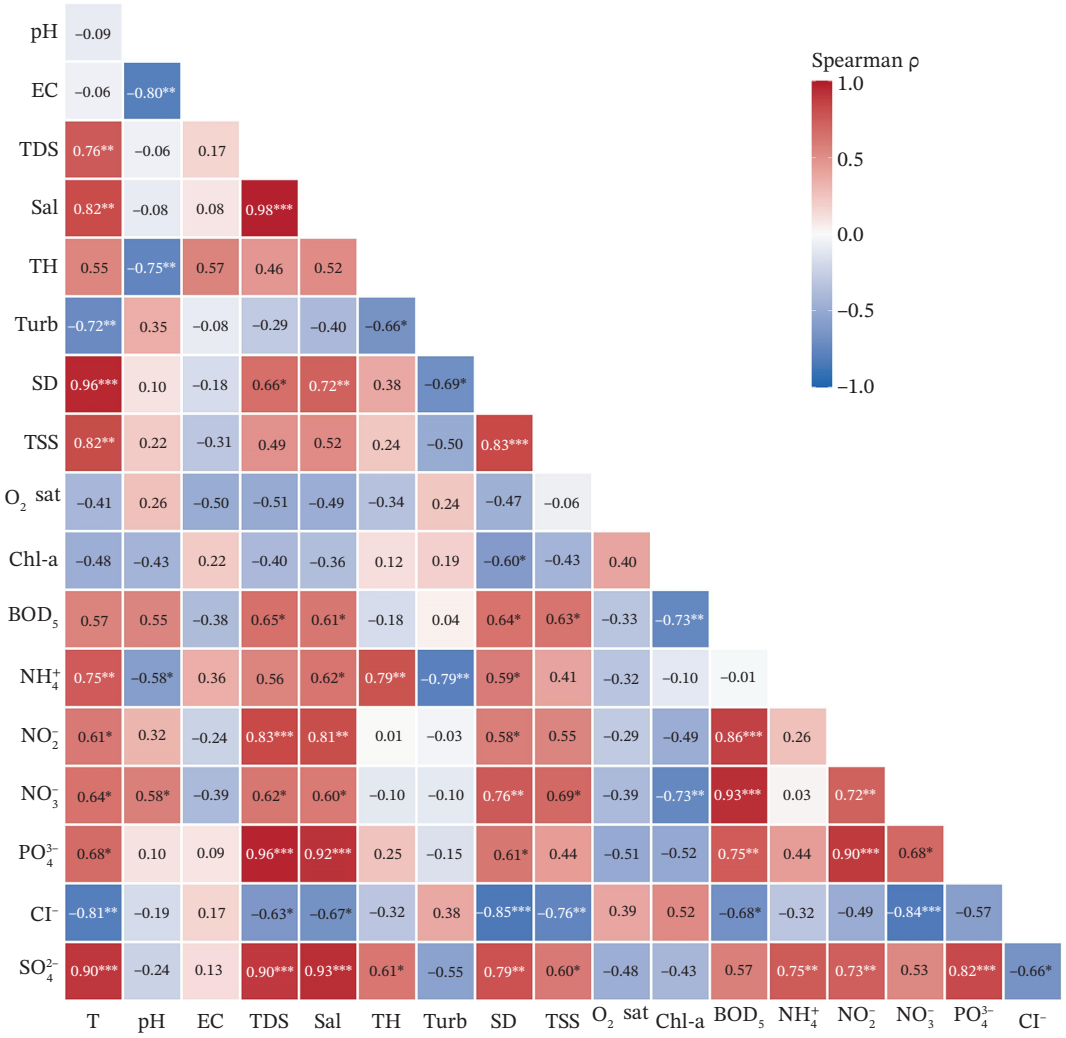

FIGURE 7 | Seasonal dynamics of nutrient limitation (TN:TP molar ratio) in the El Hamiz reservoir.

These values are well below those of Babar (up to 308.9 mg/L) [32]. Sulfate concentrations ranged from 130 to 199 mg/L in winter–spring and increased to 347–493 mg/L in summer, exceeding the 400 mg/L limit at HMZ1 and HMZ3 (PL = 1.11 and 1.23). This seasonal exceedance suggests contributions from sulfate-based fertilizers and gypsum dissolution [51]. Turbidity (4.1–30.8 NTU) exceeded the 5 NTU potability threshold in all seasonal means except summer at HMZ3 (PL up to 6.16), with peaks in winter and autumn associated with runoff inputs and sediment resuspension, and decreasing from HMZ1 toward HMZ3. Secchi depth (49–707 cm) varied widely, with the lowest values at HMZ1 associated with high turbidity and TSSs (17–194 mg/L, apart from an isolated value of 986 mg/L at HMZ2 in autumn), which limited light penetration and amplified eutrophication dynamics [52]. Taken together, these data show that El Hamiz is a mineralized (especially in summer–autumn), turbid, hard water reservoir, a profile similar to that of the Beni Haroun dams [29, 53].

Nitrate concentrations were low in winter–spring (1.4–3.2 mg/L) and increased markedly in summer and autumn (6.3–29.5 mg/L), with the highest levels at HMZ2, likely due to soil leaching and mineralization of organic matter [54–57]. They remained well below the WHO (2011) [35] limit of 50 mg/L (100% compliance), suggestive of moderate agricultural nitrogen loading. This is contrary to the Beni Haroun Dam where nitrate values (107–245 mg/L) indicate a chronic nitrogen surplus due to intensive agriculture [29]. Nitrite (0.01–0.16 mg/L, with a maximum at HMZ1) and ammonium (0.08–0.42 mg/L) levels were also within WHO limits (100% compliance); the higher ammonium concentrations recorded at all stations in summer indicate enhanced ammonification of organic matter.

Orthophosphate (PO_4^{3-}) was low in winter–spring (0.02–0.09 mg/L) but increased at HMZ1 in summer and autumn (0.29 and 0.62 mg/L), exceeding its standard only at this station in autumn (PL = 1.24). The upstream inflow is therefore the main entry point of phosphorus into the reservoir. Except for HMZ3 in spring, all orthophosphate values exceeded 0.025 mg/L, a concentration commonly used as a eutrophication threshold for TP. Since orthophosphate represents only the dissolved reactive fraction, TP concentrations are likely to be higher, which supports the conclusion of an excessive phosphorus supply to the reservoir. Comparable or higher phosphorus levels have been reported at Beni Haroun (0.045–0.598 mg/L) [29, 53], and such enrichment is widely recognized as a driver of structural

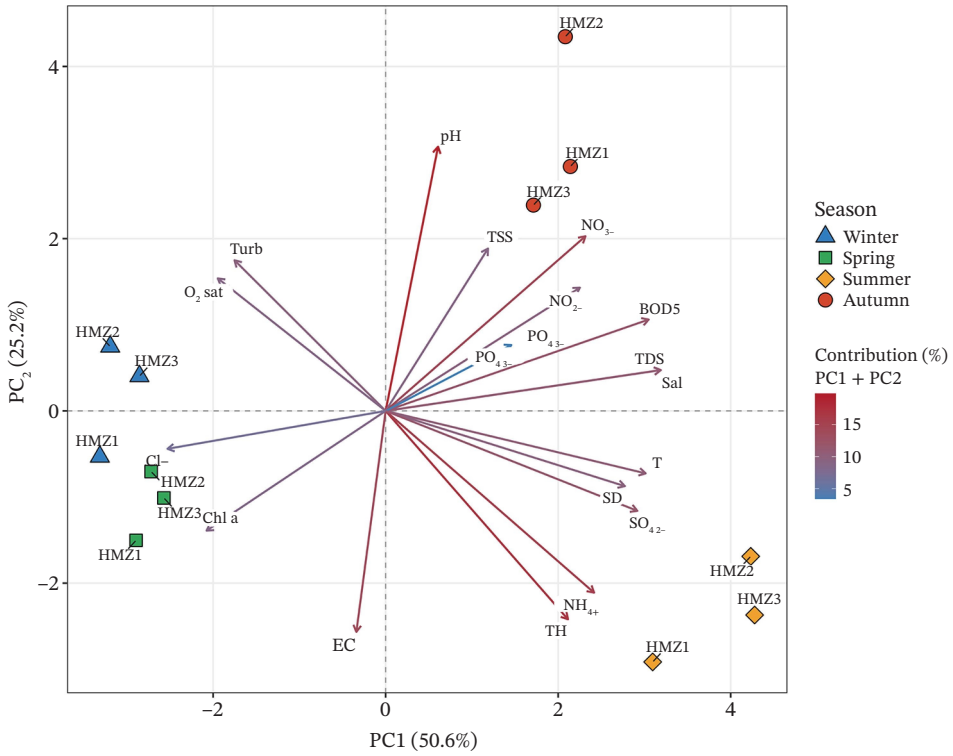

FIGURE 8 | Biplot of the principal component analysis (PC1–PC2) of the physicochemical and biological variables of the El Hamiz reservoir (2018). Symbols indicate the seasons, and labels indicate stations; arrow color indicates the contribution of each variable to the first two components.

eutrophication in Algerian reservoirs [40, 57]. This localized phosphorus signal is isolated by the third principal component, which is dominated by orthophosphate and nitrite and mainly reflects HMZ1 in summer and autumn; it explains why orthophosphate did not follow the general seasonal pattern described by the first component.

Chlorophyll a concentrations were moderate (2.1–12.4 µg/L), ranging from the mesotrophic to the eutrophic–supertrophic boundary of Burns et al. [22] (Table 5), with distinct spring peaks (up to 12.4 µg/L at HMZ3) and a summer peak at HMZ1 (11.3 µg/L), whereas lower concentrations were recorded in autumn (3.4–4.3 µg/L) and in summer at HMZ2 (≈2 µg/L). These patterns suggest algal growth favored by rising temperature and light availability in spring, followed by a seasonal decrease in phytoplankton activity [32, 58, 59]. Chl a did not differ significantly between seasons or stations ($p = 0.241$ and 0.779) and was negatively correlated with BOD_5 and nitrate ($\rho = -0.73$); i.e., algal biomass was highest in spring, before nutrient and organic concentrations reached their maximum. In the PCA, chlorophyll a lies on the negative side of PC1, opposite to BOD_5 and nitrate, which confirms that phytoplankton biomass did not follow nutrient enrichment during the dry season.

The BOD_5 values (7.1–28.1 mg/L, with 7.1–9.7 mg/L in winter–spring and 23.5–28.1 mg/L in summer–autumn, i.e., a near threefold increase) were 100% of samples above the clean-water reference of 5 mg/L, indicating seasonal organic inputs, but remained far below raw-sewage levels and considerably lower than at Ourkiss, Babar, and Timgad (BOD_5: 84.6–99.7 mg/L) [40]. COD values ranged from 8.9 to 35.1 mg/L, exceeding the 30 mg/L standard only at the highest values. The COD/BOD_5 ratio of about 1.25 reflects the predominance of biodegradable organic compounds, probably of mixed anthropogenic origin (partially treated wastewater and agroindustrial effluents) and natural origin (plant debris and phytoplankton decomposition products). The OPI calculated according to Leclercq and Maquet [10] showed a clear contrast between the cool and the warm halves of the year. In winter–spring, OPI values were between 3.25 and 3.75 at all stations (moderate organic pollution class; 50% of observations), revealing a higher degree of hydrological renewal and lower microbial respiration. In summer–autumn, OPI deteriorated to 2.00–2.50 (high organic pollution class; 50% of observations): HMZ1 reached 2.25 in summer and 2.00 in autumn (the lowest value of the annual cycle, at the limit of the very high class), while HMZ2 and HMZ3 were 2.50 in both seasons. This deterioration was mainly driven by BOD_5 (> 15 mg/L, lowest score), together with the increase in nitrite (60–160 µg/L) and, at HMZ1, in orthophosphate (290–620 µg/L), whereas ammonium contributed little to the organic load in winter–spring. The warmest seasons' worst OPI at HMZ1 is attributed to its proximity to terrestrial inputs and reduced hydrodynamic flushing. These mechanisms include microbial metabolism accelerated by temperature (Van't Hoff's law), reduced water renewal, and localized summer inputs of pollutants. Similar seasonal OPI patterns have been recorded at Hammam Grouz [60], Ain Zada [61], Beni Haroun [29], and Timgad and Ourkiss [40, 62, 63].

The WPI (Ref. [13]) ranged from 0.60 to 1.27 and showed a clear seasonal pattern combined with a consistent upstream-to-dam gradient. The seasonal mean WPI decreased from 0.90 in winter to 0.71 in spring, before rising to 1.08 in summer and 1.17 in autumn. Of the 12 seasonal observations, 50% (all in summer–autumn) were classified as highly polluted, 33% as moderately

polluted, and 17% as good (spring, HMZ2 and HMZ3); none reached the excellent class. HMZ1 recorded the highest WPI in every season (annual mean 1.08, versus 0.95 at HMZ2 and 0.87 at HMZ3), possibly indicating greater exposure to terrestrial pollution sources in the upstream zone. The contrast between stations was most pronounced in winter and spring (up to 0.27 WPI units) and weakened in summer (≤ 0.17 units). The index was controlled by a small number of variables: turbidity and TDS in winter–spring; TDS, total hardness and sulfate in summer; and TDS and turbidity, together with orthophosphate at HMZ1 and pH at HMZ2, in autumn. Nitrate, nitrite, ammonium, and chloride never exceeded their limits (PL ≤ 0.59), so the classification reflects mainly mineralization and particulate load rather than nutrient enrichment. This summer deterioration reflects findings across Algerian dams: Ourkiss was described as heavily polluted at 80% of sites in summer/autumn [29]; Babar had 75% of sites moderately to heavily polluted in the hot season [28]; Timgad was 75% heavily polluted year-round [57]; and Beni Haroun and Oued Athmania dams showed similar deterioration [29, 54]. In summer and autumn, all three stations shifted simultaneously to the highly polluted class, which supports the idea that seasonal climatic forces, such as evaporoconcentration and extended hydraulic retention, govern water quality at the reservoir scale during the dry season, whereas an upstream-to-dam gradient prevailed in the wet season [30].

The NPI provided a more severe classification than the WPI, particularly in winter. NPI values ranged from 1.25 to 4.41 (Classes III to V), with 83% of the samples (10 of 12) in Class V (heavily polluted). In winter, all stations were in Class V (3.15–4.41; HMZ1: 4.41, the highest value of the annual cycle; HMZ2: 4.12; HMZ3: 3.15), whereas the WPI indicated moderate pollution. This difference results from the structure of the Nemerow index, which gives greater weight to the most polluting parameter: a single parameter exceeding its standard several-fold (turbidity in winter) is enough to classify the water as heavily polluted, even when the average pollution load remains below 1. In spring, the NPI decreased markedly at HMZ2 (1.53) and HMZ3 (1.25), placing them in Class III (slightly polluted), whereas HMZ1 remained in Class V (3.30); in summer (3.37–3.52) and autumn (3.14–3.46), all stations were again in Class V. Pmax was controlled by only two parameters: turbidity in winter and spring ($P_i = 1.67$–6.16), reflecting runoff inputs of suspended particles, and TDS in summer ($P_i = 4.66$–4.84) and in autumn at HMZ1 and HMZ3 (turbidity at HMZ2), reflecting dry-season mineralization combined with the first autumn runoff events. Nutrients and chloride never controlled the NPI ($P_i \leq 0.59$), and PO_4^{3-} exceeded its standard only at HMZ1 in autumn ($P_i = 1.24$). Comparable Class IV–V values during thermal stress periods have been documented at Babar and Ourkiss [40], and quasi-permanent Class V conditions at Timgad.

The spatiotemporal analysis of the NPI (Table 7) revealed marked temporal variations. The winter-to-spring transition brought a significant improvement ($T\% = +47.94\%$; mean NPI from 3.89 to 2.03), related to the decrease in turbidity once the winter runoff ended. It was followed by a significant deterioration from spring to summer ($T\% = -69.07\%$; mean NPI 3.43), coinciding with the dry season, when TDS became the parameter with the highest pollution index at all stations. Between summer and autumn, the NPI hardly changed ($+2.30\%$, $< 10\%$), and the autumn-to-winter transition showed a moderate deterioration (-16.29%), the mean NPI reaching its annual maximum in winter (3.89) under high turbidity linked to runoff and sediment inputs. The reservoir therefore does not recover during the wet season: Spring is the most favorable period, whereas winter and summer are the most critical, for different reasons (particulate inputs in winter, mineralization in summer). Spatially, water quality was clearly heterogeneous in winter and spring ($S\% = 28.50\%$ and 62.11%), with the NPI decreasing from HMZ1 toward the dam, reflecting the role of the upstream zone as the main entry point of turbid runoff water, the suspended particles settling progressively along the reservoir. In summer and autumn, the spatial variability was low ($S\% = 4.29\%$ and 9.29%, $< 10\%$), indicating that the three stations were affected in a similar way by processes acting at the scale of the whole water body. El Hamiz thus behaves as a spatially heterogeneous system during the wet season and becomes almost uniform during the dry season. This strong seasonal contrast is consistent with that documented at Beni Haroun and Oued Athmania [29].

The trophic status assessed with the TLI remained high throughout the year, with values between 4.65 and 5.94, i.e., eutrophic to supertrophic in all seasons: Two-thirds of the observations fell in the supertrophic class, the remaining third in the eutrophic class, and none reached the hypertrophic threshold of 6 [22]. On a seasonal basis, the mean TLI was lowest in spring (4.93), followed by winter (5.07) and summer (5.23), and highest in autumn (5.66), when the three stations were all supertrophic (5.43–5.94). The slight decrease in spring is probably due to dilution by seasonal inflows, while the increase in summer–autumn is in line with higher temperatures and reduced water renewal. Spatially, the index decreased from the inflow toward the dam in every season (annual means: 5.54 at HMZ1, 5.17 at HMZ2 and 4.96 at HMZ3), and the difference between stations within a season never exceeded 0.8 units. Enrichment therefore concerns the whole water body but is more pronounced near the inflow.

This classification is not exceptional in the Algerian and regional context: the Timgad Dam showed hypertrophic status at 80% of the stations [57]; Mexa and Cheffia oscillate between eutrophic and hypertrophic states, particularly in summer [40]; even the Yabous Dam, in a less anthropized environment, has 55% hypertrophic status [37]. Comparable situations are reported in South Africa [64], Morocco [58] and subhumid Brazil [65]. El Hamiz, classified as eutrophic to supertrophic, is therefore close to, although slightly less enriched than, these reservoirs. Two synergistic enrichment sources are likely as follows: (1) agricultural runoff with huge N and P exports linked to intensive use of NPK and manure during rainfall events [51, 66]; and (2) domestic wastewater from upstream urban areas with poor sanitation infrastructure, which release N- and P-rich effluents [63]. The contribution of internal sediment recycling could not be assessed, since only surface samples were collected.

Analysis of the molar ratio of TN:TP [67] showed a spatially differentiated nutrient limitation regime. At the littoral HMZ1 station, the ratio was transitional throughout the year (winter: 28.78; spring: 20.14; summer: 22.18; autumn: 22.88; reference range 20–50), indicating variable watershed inputs, rapid water–sediment exchange, and resuspension processes constantly changing N:P ratios. In the pelagic zone (HMZ2), phosphorus limitation was dominant in winter (TN:TP = 51.53), a short

nitrogen limitation episode occurred in spring (TN:TP = 19.39), and high ratios in summer (132.09) and autumn (309.63) indicated potential phosphorus limitation. The embankment zone (HMZ3) showed ratios indicative of phosphorus limitation in all seasons: winter (104.62), spring (71.29), summer (119.55), and autumn (243.60). Phosphorus limitation in summer and autumn may be related to two interrelated processes: (a) sedimentation of particulate P, and (b) rapid uptake of bioavailable P by algal blooms. Thermal stratification isolating P-rich deep waters from the euphotic zone [33] is a possible additional mechanism, but it cannot be confirmed here because no depth profiles were collected. The limited availability of nitrogen in spring at HMZ2 could be caused by phosphorus inputs in spring runoff or by a community of algae that consume nitrogen preferentially [68]. These results are consistent with Babar and Ourkiss where phosphorus is also the primary limiting nutrient in open waters [40]. The very high ratios (> 100, up to 309.63) should be interpreted with caution, as they may reflect TP concentrations close to the detection limit. The most efficient strategy for the reversal of lake eutrophication is phosphorus control as shown by Schindler et al. [69].

The Friedman test confirmed that most of the variability in the reservoir was seasonal: 14 of the 18 variables differed significantly between seasons ($p < 0.05$), versus only seven between stations (temperature, EC, TDS, turbidity, transparency, TSS, and oxygen saturation), mostly linked to suspended particles and light penetration, consistent with the gradient between the turbid inflow zone at HMZ1 and the clearer water near the Dam. Nutrients, organic load and chlorophyll a did not vary significantly between stations, although with three stations and four seasons, the power of the test is limited and a nonsignificant result does not necessarily mean that the stations were identical. The Spearman correlations ($n = 12$) mostly followed the seasonal cycle: Temperature was closely related to transparency ($\rho = 0.96$) and sulfate (0.90); BOD_5 increased together with nitrate (0.93) and nitrite (0.86), and nitrite was closely linked to orthophosphate (0.90), showing that organic load and nutrient enrichment developed together during the warm season. Given the small number of observations, these coefficients describe shared seasonal patterns more than direct causal links.

The PCA supports these results and adds information on the processes involved. The first component (50.6% of the variance) opposes the dry-season conditions, with higher temperature, mineralization, organic load, and nutrients in clearer water, to the wet-season conditions, with higher turbidity, oxygen saturation, chloride, and chlorophyll a. The second component (25.2%) separates summer from autumn (Figure 8). Summer samples were associated with hardness, ammonium, and EC, which reflects the accumulation of dissolved salts and the decomposition of organic matter in warm, slowly renewed water. Autumn samples were associated with pH, nitrate, TSS, and turbidity, consistent with the nitrification of the ammonium accumulated in summer and with the first runoff events. Summer and autumn, although both belonging to the degraded period, are therefore governed by different processes. The third component (9.8%) is dominated by orthophosphate and nitrite and mainly reflects HMZ1 in summer and autumn, which confirms the role of the inflow zone as the main entry point of phosphorus. Within each season, the three stations remained close together on the factorial plane, in agreement with the Friedman test, which found many more seasonal than spatial differences. Winter and spring samples formed a single group, which indicates that the two wet-season periods are chemically similar, although winter samples lay slightly closer to turbidity and oxygen saturation. With twelve samples for eighteen variables, the PCA remains a descriptive tool, but its structure is consistent with the statistical tests and with the pollution indices (Figure S3).

An integrated analysis of all five indices (WPI, NPI, OPI, TLI, and TN:TP) delivers a consistent diagnosis. El Hamiz reservoir exhibits a pronounced seasonal water quality regime with two critical periods: winter, when runoff brings turbidity and particulate inputs and the NPI places all stations in Class V, and summer–autumn, when water quality deteriorates at all stations (WPI > 1, high organic pollution class, TLI up to 5.94). Eutrophic-to-supertrophic conditions persist throughout the year. The NPI placed 10 of 12 observations in Class V, controlled by turbidity in winter–spring and TDS in summer–autumn rather than by nutrients. The PCA explains this result: TDS and turbidity, the two parameters responsible for Pmax, lie on opposite sides of the first component so that each season has its own source of degradation. The main driver is the subhumid Mediterranean climate cycle: Wet-season runoff brings turbidity and particulate inputs, while dry-season mineralization and prolonged hydraulic residence times amplify anthropogenic pressures (agricultural runoff and inadequately treated urban discharges). The upstream-to-dam gradient observed in the wet season (S% = 28.50%–62.11%) disappears in the dry season ($S\% < 10\%$). Management must therefore give particular attention to the inflow zone (HMZ1) during the wet season, while operating at the reservoir and watershed scales during the dry season.

This study has limitations: Samples were collected monthly at three stations and only at the surface (30 cm), the monthly data were aggregated seasonally (one value per station and season), and no depth profiles were available. Stratification, hypolimnetic oxygen depletion, and internal phosphorus loading could therefore not be assessed, and the statistical power was limited.

This ecological dynamic is shared by a set of Algerian and Mediterranean reservoirs, namely, Babar and Ourkiss [40], Beni Haroun and Oued Athmania [29], Timgad [57], and internationally comparable systems in South Africa [64], Morocco [58], and semiarid Brazil [65]. Four management interventions are suggested: (i) modernize wastewater treatment infrastructure to achieve tertiary phosphorus removal for urban effluents entering the catchment; (ii) establish buffer strips and constructed wetlands to intercept diffuse agricultural phosphorus runoff, together with sediment-retention measures at the inflow of the main Oued, since turbidity was the main driver of winter–spring pollution; (iii) deploy a monitoring network targeted on the critical periods identified here, with turbidity and suspended solids followed closely during the wet season and BOD_5, nutrients and chlorophyll a during summer–autumn so that early signs of phytoplankton blooms can be detected; and (iv) use the indices applied in this study, which are simple to compute, as alert thresholds and, in the longer term, combine them with predictive modeling tools to anticipate quality crises [26, 40]. Given the urgency, monitoring should be given priority and implemented at a much finer spatiotemporal resolution than in

the present study (weekly to biweekly sampling during the spring-to-autumn period, additional stations or continuous sensors at the inflow, and depth-resolved profiles), as a prerequisite for the medium- and long-term measures. These suggestions are aligned with the integrated management approaches presented by Chorus and Bartram [59], and Uslu et al. [31] for reservoirs serving dual drinking water and irrigation functions under increasing climatic and anthropogenic stresses.

5 | Conclusion

This study provides the first integrated assessment of water quality in El Hamiz Dam by combining five indices (WPI, NPI, OPI, TLI, and TN:TP) with multivariate statistics. The results reveal a pronounced seasonal regime driven mainly by turbidity in the wet season and mineralization in the dry season. The WPI ranged from 0.60 to 1.27, with seasonal means of 0.90 in winter, 0.71 in spring, 1.08 in summer, and 1.17 in autumn; 50% of the 12 seasonal observations were highly polluted, 33% moderately polluted, and 17% good, and none was excellent. The NPI ranged from 1.25 to 4.41, and 10 of 12 samples (83%) fell in Class V (heavily polluted). Only spring at HMZ2 (1.53) and HMZ3 (1.25) was slightly polluted (Class III). The NPI was controlled by only two parameters. P_{max} was associated with turbidity in winter and spring ($P_i = 1.67–6.16$, maximum at HMZ1 in winter) and with TDS in summer ($P_i = 4.66–4.84$), and then with TDS at HMZ1 (4.73) and HMZ3 (4.32) and turbidity at HMZ2 (4.72) in autumn. Nitrate, nitrite, ammonium, and chloride never exceeded their standards ($P_i \leq 0.59$), and orthophosphate exceeded its limit only at HMZ1 in autumn ($P_i = 1.24$). Mineralization increased sharply from winter–spring to summer–autumn:

The persistent hypertrophic state and systematic warm-season degradation underscore the urgent need for adaptive management. Four interventions are recommended: (i) Modernize wastewater treatment for tertiary phosphorus removal; (ii) establish buffer strips and constructed wetlands to intercept agricultural runoff; (iii) deploy real-time monitoring for early cyanobacterial bloom warnings during summer and autumn; and (iv) integrate predictive modeling tools to anticipate quality crises.

Given the urgency of the water quality deterioration observed in the El Hamiz reservoir, immediate action should also focus on intensifying monitoring at shorter temporal intervals and across a more detailed spatial sampling network. More frequent sampling, particularly during the spring–summer transition and throughout summer and autumn, would help capture rapid changes in water quality, identify pollution peaks, and provide earlier warnings of potential cyanobacterial blooms. This intensified monitoring should complement the proposed medium- and long-term management measures and support timely, evidence-based interventions to protect the reservoir ecosystem and its water uses [70–72].

Author Contributions

Amin Chaffai and Hichem Khammar designed the study, conducted field sampling, and wrote the manuscript. Nadhir Bouchema performed the data analysis.

Acknowledgments

The authors acknowledge the Babar Dam management authority for providing site access and the Laboratory of Functional Ecology and Environment, University of Oum El Bouaghi, Algeria (LEFE), for analytical facilities.

Funding

This research received no specific grant from any public, commercial, or not-for-profit funding agencies.

Conflicts of Interest

The authors declare no conflicts of interest.

Data Availability Statement

The physicochemical and water quality datasets supporting this study are available from the corresponding author upon reasonable request (hichem.khammar@univ-oeb.dz).

References

1. A. Mezhoud, H. Khammar, N. Bouchema, A. Chaffai, and A. Ouldjaoui, "Hydrogeochemical and Hydrochemical Evaluation of Surface Water: Insights Into Water Quality For Drinking Use," *Studies in Engineering and Exact Sciences* 5 (2024): https://doi.org/10.54021/seesv5n3-047.

2. K. Tockner and J. J. Bogardi, eds., in *Handbook of Water Resources Management: Discourses, Concepts and Examples* (Springer, 2021), https://doi.org/10.1007/978-3-030-60147-8_16.

3. J. S. Albert, G. Destouni, S. M. Duke-Sylvester, et al., "Scientists' Warning to Humanity on the Freshwater Biodiversity Crisis," *Ambio* 50, no. 1 (2020): 85–94, https://doi.org/10.1007/s13280-020-01318-8.

4. A. Chaffai, S. Hamil, I. Adaouri, S. Arab, A. Moussouni, and A. Arab, "Factors Determining Phytoplankton Community Growth and Succession in the Water's Surface of Mediterranean Reservoir," *Biodiversity Journal* 13, no. 1 (2022): 55–64, https://doi.org/10.31396/Biodiv.Jour.2022.13.1.55.64.

5. C. Belaroussi, "Changes in Population Structure in Algeria," *RIMAK International Journal of Humanities and Social Sciences* 6, no. 3 (2024): 1060–1070, https://doi.org/10.47832/2717-8293.29.25.

6. N. Turini, B. Thies, and J. Bendix, "Estimating High Spatio-Temporal Resolution Rainfall From MSG1 and GPM IMERG Based on Machine Learning: Case Study of Iran," *Remote Sensing* 11, no. 19 (2019): 2307, https://doi.org/10.3390/rs11192307.

7. C. Fehdi, A. Rouabhia, F. Baali, and A. Boudoukha, "The Hydrogeochemical Characterization of Morsott-El AOUINET Aquifer, Northeastern Algeria," *Environmental Geology* 58, no. 7 (2009): 593–603, https://doi.org/10.1007/s00254-008-1667-4.

8. A. Hamad, I. Abdeslam, C. Fehdi, et al., "Vulnerability Characterization for Multi-Carbonate Aquifer Systems in Semiarid Climate, Case of Algerian–Tunisian Transboundary Basin," *International Journal of Energy and Water Resources* 6, no. 1 (2022): 67–80, https://doi.org/10.1007/s42108-021-00142-4.

9. A. Khalaf Ahmed Albaggar, "Investigation of Some Physical, Chemical, and Bacteriological Parameters of Water Quality in Some Dams in Albaha Region, Saudi Arabia," *Saudi Journal of Biological Sciences* 28, no. 8 (2021): 4605–4612, https://doi.org/10.1016/j.sjbs.2021.04.067.

10. L. Leclercq and B. Maquet, "Documents De Travail De L'Institut Royal Des Sciences Naturelles De Belgique," *Studiedocumenten van het Koninklijk Belgisch Instituut voor Natuurwetenschappen* 38 (1987): 1–113.

11. L. Leclercq and L. Vandevenne, "Macroecological Patterns of Genetic Structure and Diversity in the Aquatic Moss Platyhypnidium Riparioides," *Cahiers De Biologie Marine* 28, no. 2 (1987): 311–318.

12. H. S. Al-Nuaimi and A. A. Murad, "The Role of Dams in Securing the Surface Water in the Northern and Eastern Parts of the United Arab Emirates (UAE)," *Tunnelling and Underground Space Technology* 18 (2007).

13. M. Hossain and P. K. Patra, "Water Pollution Index–a New Integrated Approach to Rank Water Quality," *Ecological Indicators* 117 (2020): https://doi.org/10.1016/j.ecolind.2020.106668.

14. B. O. Isiuku and C. E. Enyoh, "Pollution and Health Risks Assessment of Nitrate and Phosphate Concentrations in Water Bodies in South Eastern, Nigeria," *Environmental Advances* 2 (2020): https://doi.org/10.1016/j.envadv.2020.100018.

15. G. Klippel, R. L. Macêdo, and C. W. C. Branco, "Lakes and Reservoirs: Science," *Policy and Management for Sustainable Use* 25, no. 2 (2020): 214–229, https://doi.org/10.1111/lre.12320.

16. C. Tokatli, "Application of Nutrient Pollution Index and Water Pollution Index to Evaluate the Drinking Water Quality of the Villages Located In Edirne, Turkey," in *International Agricultural, Biological & Life Science Conference* (2021).

17. H. Ali, R. Boualem, and R. Mohamed, "Numerical Modelling of Solid Transport Caused by an Extreme Flood: Case of the Hamiz Dam Failure (Algeria)," *Journal of King Saud University-Engineering Sciences* 29, no. 3 (2017): 221–236, https://doi.org/10.1016/j.jksues.2014.08.003.

18. J. Rodier, B. Legube, and N. Merlet, *L'analyse de L'eau: Eaux Naturelles, Eaux Résiduaires, Eau De Mer*, 9th ed. (Dunod, 2009).

19. N. L. Nemerow, *Scientific Stream Pollution Analysis* (Scripta Book Company, 1974).

20. K. Su, Q. Wang, L. Li, R. Cao, Y. Xi, and G. Li, "Water Quality Assessment Based on Nemerow Pollution Index Method: A Case Study of Heilongtan Reservoir in Central Sichuan Province, China," *PLoS One* 17, no. 8 (2022): e0273305, https://doi.org/10.1371/journal.pone.0273305.

21. K. Su, Q. Wang, R. Cao, Z. Peng, Y. Xi, and G. Li, "Water Quality Assessment and Spatial-Temporal Change: the Case of Zipingpu Reservoir in Central Sichuan Province, China," *Environmental Quality Management* 33, no. 4 (2024): 835–842, https://doi.org/10.1002/tqem.22160.

22. N. Burns, J. McIntosh, and P. Scholes, "Trophic Status Analysis and Nutrient Source Allocation in Urban Lakes of Dhaka, Bangladesh: A Comprehensive Approach to Eutrophication Monitoring," *Lake and Reservoir Management* 15, no. 4 (1999): 255–271, https://doi.org/10.1080/07438149909354122.

23. S. J. Guildford and R. E. Hecky, "Total Nitrogen, Total Phosphorus, and Nutrient Limitation in Lakes and Oceans: Is There a Common Relationship?" *Limnology and Oceanography* 45, no. 6 (2000): 1213–1223, https://doi.org/10.4319/lo.2000.45.6.1213.

24. R Core Team, *R: A Language and Environment for Statistical Computing* (R Foundation for Statistical Computing, 2025), https://www.R-project.org/.

25. S. M. Liou, S. L. Lo, and S. H. Wang, "A Generalized Water Quality Index for Taiwan," *Environmental Modeling & Assessment* 96, no. 1–3 (2004): 35–52, https://doi.org/10.1023/b:emas.0000031715.83752.a1.

26. R. Noori, R. I. Woolway, C. Jun, S. M. Bateni, M. Maghrebi, and M. Pulkkanen, *Multi-Decadal Change in Summer Mean Water Temperature in Lake Konnevesi* (Finland, 2022), 1984–2021, https://doi.org/10.21203/rs.3.rs-1982578/v1.

27. A. Gaagai, K. Lasri, and H. Khammar, "Physico-Chemical and Toxicological Characteristics of Leachates From MSW Landfills," *Polish Journal of Environmental Studies* 29, no. 4 (2020): 2571–2582.

28. A. Gaagai, H. A. Aouissi, and S. E. Maalem, "Impact of Climate Change and Anthropic Activity on The Water Quality of Babar Dam in Algeria," *Global Journal of Engineering Sciences* 6, no. 4 (2020): https://doi.org/10.33552/gjes.2020.06.00064.

29. N. Bouchareb, "Experimental Versus Theoretical Study of Reverse Osmosis Pilot Scaling: The Case of Algerian Brackish Water Desalination," *Journal of Water and Land Development* 62 (2024): 45–58.

30. S. Chidiac, P. El Najjar, N. Ouaini, Y. El Rayess, and D. El Azzi, "A Comprehensive Review of Water Quality Indices (WQIs): History, Models, Attempts and Perspectives," *Reviews in Environmental Science and Bio/Technology* 22, no. 2 (2023): 349–395, https://doi.org/10.1007/s11157-023-09650-7.

31. G. Uslu, B. Taş, and A. Çiçek, "Trading Behavior-Stock Market Volatility Nexus Among Institutional and Individual Investors," *Journal of Environmental Management* 356 (2024).

32. A. Gaagai, L. Bouzidi, and H. Khammar, "Water Treatment and Desalination," *Environmental Science, Engineering* 87 (2017): 183–192.

33. I. Kagalou, E. Papastergiadou, and I. Leonardos, "Long Term Changes in the Eutrophication Process in a Shallow Mediterranean Lake Ecosystem of W. Greece: Response After the Reduction of External Load," *Journal of Environmental Management* 87, no. 3 (2008): 497–506, https://doi.org/10.1016/j.jenvman.2007.01.039.

34. M. Touzani, O. Machkor, I. Boudouch, El Machrafi, R. Flouchi, and K. Fikri-Benbrahim, "Environmental Impact Assessment of Taza City's Wastewater: Application Through Principal Component Analysis," *Scientific* 2020 (2020): 1–7, https://doi.org/10.1155/2020/9168569.

35. WHO, *Guidelines for Drinking-water Quality*, 4th ed. (World Health Organization, 2011).

36. S. Bouslah and L. Djemili, "Water Quality Index Assessment of Koudiat Medouar Reservoir,Northeast Algeria Using Weighted Arithmetic Index Method," *Journal of Water and Land Development* 35, no. 1 (2017): 221–228, https://doi.org/10.1515/jwld-2017-0087.

37. N. Bouchema, H. Khammar, S. Nadjai, B. Tellil, and Z. Zeghdani, "Assessment of Surface Water Quality for Drinking and Irrigation Purposes for Two Dams in the Semi-Arid Region of Northeast Algeria," *Global NEST Journal* 26, no. 8 (2024): https://doi.org/10.30955/gnj.05912.

38. J. Wu, P. Li, D. Wang, X. Ren, and M. Wei, "Statistical and Multivariate Statistical Techniques to Trace the Sources and Affecting Factors of Groundwater Pollution in a Rapidly Growing City on the Chinese Loess Plateau," *Human and Ecological Risk Assessment: An International Journal* 26, no. 6 (2019): 1603–1621, https://doi.org/10.1080/10807039.2019.1594156.

39. C. Apollaro, D. Di Curzio, I. Fuoco, et al., "A Multivariate Non-Parametric Approach for Estimating Probability of Exceeding the Local Natural Background Level of Arsenic in the Aquifers of Calabria Region (Southern Italy)," *Science of the Total Environment* 806 (2022): https://doi.org/10.1016/j.scitotenv.2021.150345.

40. Z. Sahraoui, H. Khammar, S. Nadjai, A. Chaffai, N. Bouchema, and A. Bourmada, "Assessment of Water Quality in Two Dams in Semi-Arid Region Dams of Northeastern Algeria: Using Pollution Indices," *Global NEST Journal* (2025): https://doi.org/10.30955/gnj.07034.

41. B. Nas, A. Berktay, A. Aygun, H. Karabork, and S. Ekercin, "Turkey," *Environmental Technology* 30, no. 4 (2009): 345–353, https://doi.org/10.1080/09593330902752984.

42. N. Pacini, K. Donabaum, P. Henry de Villeneuve, et al., "Water-Quality Management in a Vulnerable Large River: The Nile in Egypt," *International Journal of River Basin Management* 11, no. 2 (2013): 205–219, https://doi.org/10.1080/15715124.2013.781032.

43. N. Subba Rao, D. Marghade, A. Dinakar, et al., "Geochemical Characteristics and Controlling Factors of Chemical Composition of Groundwater in a Part of Guntur District, Andhra Pradesh, India," *Environmental Earth Sciences* 76 (2017): 1–22, https://doi.org/10.1007/s12665-017-7093-8.

44. R. Das Kangabam, M. Govindaraju, S. Meenakshi, and S. Prasad, "Development of a Water Quality Index (WQI) for the Loktak Lake in

India," *Applied Water Science* 7, no. 6 (2017): 2907–2918, https://doi.org/10.1007/s13201-017-0579-4.

45. A. Merouche, S. Selvam, Y. Imessaoudene, and C. N. Maten, "Assessment of Dam Water Quality for Irrigation in the Northeast of Catchment Cheliff-Zahrez, Central Algeria," *Environment, Development and Sustainability* 22, no. 6 (2021): 5709–5730, https://doi.org/10.1007/s10668-019-00447-9.

46. M. Ouhmidou and A. Chahlaoui, "Physico-Chemical Quality of the Water of the Hassan Addakhil Dam of Errachidia-Morocco," *Science Lib Editions Mersenne* 5 (2013): http://eprints.umi.ac.ma/id/eprint/939.

47. Z. C. Koudenoukpo, D. Chikou, R. Hazoume, I. Youssao, G. A. Mensah, and A. P. Laleye, "Caractérisation Physico-Chimique D'un Système Lotique en Région Tropicale: La Rivière Sô au Sud-Bénin, Afrique de l'Ouest," *Journal of Applied Biosciences* 113, no. 1 (2017): 11111–11122, https://doi.org/10.4314/jab.v113i1.1.

48. R. E. Turner and N. N. Rabalais, "Linking Landscape and Water Quality in the Mississippi River Basin for 200 Years," *BioScience* 53, no. 6 (2003): 563–572.

49. K. L. Oliveira, R. L. Ramos, S. C. Oliveira, et al., "Spatial Variability of Surface Water Quality in a Large Brazilian Semiarid Reservoir and its Main Tributaries," *Environmental Monitoring and Assessment* 193 (2021): 409, https://doi.org/10.1007/s10661-021-09194-9.

50. E. Derwich, Z. Beziane, L. Benaabidate, and D. Belghyti, "Evaluation De La Qualite Des Eaux De Surface Des Oueds Fes Et Sebou Utilisees En Agriculture Maraichere Au Maroc," *Larhyss Journal* 7, no. 1 (2008): 59–77, https://asjp.cerist.dz/en/article/54797.

51. N. U. Kura, M. F. Ramli, S. Ibrahim, W. N. A. Sulaiman, and A. Z. Aris, "An Integrated Assessment of Seawater Intrusion in a Small Tropical Island Using Geophysical, Geochemical, and Geostatistical Techniques," *Environmental Science and Pollution Research* 21, no. 11 (2014): 7047–7064, https://doi.org/10.1007/s11356-014-2598-0.

52. R. G. Wetzel, *Limnology: Lake and River Ecosystems*, 3rd ed. (Academic Press, 2001).

53. S. Bouaroudj, A. Bouasla, F. Bouchetat, A. C. Rebbah, N. Bouchareb, and A. Bounamous, "Assessment of Roadside Potentially Toxic Metal Contamination Using Linum usitatissimum L. as a Bioindicator in Sargodha, Pakistan," *Global NEST Journal* 27, no. 2 (2025): 1–8, https://doi.org/10.30955/gnj.06523.

54. A. Bouderbala, S. Boutaleb, and N. Akkal, "Occurrence, Environmental Impact and Fate of Pharmaceuticals in Groundwater and Surface Water: A Critical Review," *Environmental Science and Pollution Research* 27 (2020): 14551–14568.

55. S. Hamil, S. Arab, A. Chaffai, M. Baha, and A. Arab, "Assessment of Surface Water Quality Using Multivariate Statistical Analysis Techniques: A Case Study From Ghrib Dam, Algeria," *Arabian Journal of Geosciences* 11, no. 23 (2018): 754, https://doi.org/10.1007/s12517-018-4102-5.

56. R. H. Kadlec and S. D. Wallace, *Treatment Wetlands*, 2nd ed. (CRC Press, 2009).

57. Z. Boudjellab, M. Ghannam, and B. Soumati, "Influence of the Thermal Stratification on the Water Quality of the Cheffia Reservoir (North-East Algeria)," *Journal of Applied Environmental and Biological Sciences* 7, no. 9 (2017): 47–58, https://www.researchgate.net/publication/364844529.

58. A. Hamid, S. U. Bhat, and A. Jehangir, "Local Determinants Influencing Stream Water Quality," *Applied Water Science* 10, no. 1 (2020): 24, https://doi.org/10.1007/s13201-019-1043-4.

59. I. Chorus and J. Bartram, eds., *Toxic Cyanobacteria in Water* (E&FN Spon, 1999).

60. B. Saadali, A. Khedidja, N. Mihoubi, A. Ouddah, T. Djebassi, and Y. Kouba, "Water Quality Assessment and Organic Pollution Identification of Hammam-Grouz Dam (Northeastern Algeria)," *Arabian Journal of Geosciences* 13, no. 20 (2020): 1091, https://doi.org/10.1007/s12517-020-06117-9.

61. A. Mebarkia, A. Haouchine, A. Boudoukha, and R. Nedjai, "Surgical Implications of Biomechanics of the Foot and Ankle," *Journal of Fundamental and Applied Sciences* 9, no. 3 (2017): 1358–1377, https://doi.org/10.4314/jfas.v9i3.8.

62. R. Mezbour, A. Reggam, M. C. Maazi, and M. Houhamdi, "Evaluation of Organic Pollution Index and the Bacteriological Quality of the Water of the Lake of Birds (ELTarf East-Algerian)," *Journal of Materials and Environmental Science* 9, no. 3 (2018): 971–979, https://doi.org/10.26872/jmes.2018.9.3.108.

63. L. Prathumratana, S. Sthiannopkao, and K. W. Kim, "The Relationship of Climatic and Hydrological Parameters to Surface Water Quality in the Lower Mekong River," *Environment International* 34, no. 6 (2008): 860–866, https://doi.org/10.1016/j.envint.2007.10.011.

64. M. D. Matlala, "Multivariate Analysis of the Dynamics in Water Quality and Trophic Status of the Crocodile River and Hartbeespoort Dam," *Environment and Ecology Research* 11, no. 1 (2023): 42–64, https://doi.org/10.13189/eer.2023.110104.

65. M. C. Wiegand, A. T. P. Nascimento, A. C. Costa, and I. E. L. Neto, "Phosphorus Mass Balance and Input Load Estimation From the Wet and Dry Periods in Tropical Semiarid Reservoirs," *Journal of Arid Environments* 184 (2021): https://doi.org/10.1016/j.jaridenv.2020.104321.

66. S. Guergazi, *Influence De La Minéralisation Sur L'Action D'Oxydants vis-à-vis De La Matière Organique Des Eaux Naturelles* (Université Mohamed Khider-Biskra, 2006).

67. J. A. Downing and E. McCauley, "The Nitrogen: Phosphorus Relationship in Lakes," *Limnology and Oceanography* 37, no. 5 (1992): 936–945, https://doi.org/10.4319/lo.1992.37.5.0936.

68. B. T. Hart and R. Harding, "Guinea Pig Models for Translation of the Developmental Origins of Health and Disease Hypothesis Into the Clinic," *Environmental Science and Technology* 49, no. 11 (2015): 6406–6415.

69. D. W. Schindler, R. E. Hecky, and G. K. McCullough, "The Rapid Eutrophication of Lake Winnipeg: Greening Under Global Change," *Journal of Great Lakes Research* 38, no. 3 (2012): 6–13, https://doi.org/10.1016/j.jglr.2012.04.003.

70. W. Geller, K. Friese, P. Herzsprung, R. Kringel, and M. Schultze, "Limnology of Sulphur-Acidic Lignite Mining Lakes. II. Chemical Main Constituents and Buffering Systems," *Internationale Vereinigung für Theoretische und Angewandte Limnologie: Verhandlungen* 27, no. 4 (2000): 2475–2479, https://doi.org/10.1080/03680770.1998.11901686.

71. J. H. Olive, *Chemical-Physical and Biological Assessment of Water Quality in the Cuyahoga River (1973-1974)* (1976).

72. B. Wang, C. Q. Liu, F. Wang, X. L. Liu, and Z. L. Wang, "A Decrease in pH Downstream From the Hydroelectric Dam in Relation to the Carbon Biogeochemical Cycle," *Environmental Earth Sciences* 73, no. 9 (2015): 5299–5306, https://doi.org/10.1007/s12665-014-3779-3.

Supporting Information

Additional supporting information can be found online in the Supporting Information section. **Supporting Information.** Supporting Tables S1 and S2 present, respectively, the pollution loads (PLi = Ci/Si) of the eleven parameters used for the WPI and the scores of the four parameters used for the OPI, as seasonal means for 2018 at the three stations of the El Hamiz reservoir. Figure S1 shows the single-factor pollution indices (Pi), Pavg and Pmax at the three stations, with the black frame marking the parameter responsible for Pmax in each sample. Figure S2 displays the Spearman rank correlation matrix of the physicochemical and biological variables ($n = 12$), and Figure S3 presents the eigenvalues (scree plot) of the PCA used to determine the number of retained components.